

1 Secondary Organic Aerosols from Anthropogenic Volatile Organic Compounds Contribute 2 Substantially to Air Pollution Mortality

3

4 Benjamin A. Nault^{1,2,*}, Duseong S. Jo^{1,2}, Brian C. McDonald^{2,3}, Pedro Campuzano-Jost^{1,2}, Douglas A.
5 Day^{1,2}, Weiwei Hu^{1,2,**}, Jason C. Schroder^{1,2,***}, James Allan^{4,5}, Donald R. Blake⁶, Manjula R.
6 Canagaratna⁷, Hugh Coe⁵, Matthew M. Coggon^{2,3}, Peter F. DeCarlo⁸, Glenn S. Diskin⁹, Rachel
7 Dunmore¹⁰, Frank Flocke¹¹, Alan Fried¹², Jessica B. Gilman³, Georgios Gkatzelis^{2,3,****}, Jacqui F.
8 Hamilton¹⁰, Thomas F. Hanisco¹³, Patrick L. Hayes¹⁴, Daven K. Henze¹⁵, Alma Hodzic^{11,16}, James
9 Hopkins^{10,17}, Min Hu¹⁸, L. Gregory Huey¹⁹, B. Thomas Jobson²⁰, William C. Kuster^{3,*****}, Alastair
10 Lewis^{10,17}, Meng Li^{2,3}, Jin Liao^{13,21}, M. Omar Nawaz¹⁵, Ilana B. Pollack²², Jeffrey Peischl^{2,3}, Bernhard
11 Rappenglück²³, Claire E. Reeves²⁴, Dirk Richter¹², James M. Roberts³, Thomas B. Ryerson^{3,*****}, Min
12 Shao²⁵, Jacob M. Sommers^{14,26}, James Walega¹², Carsten Warneke^{2,3}, Petter Weibring¹², Glenn M.
13 Wolfe^{13,27}, Dominique E. Young^{5,*****}, Bin Yuan²⁵, Qiang Zhang²⁸, Joost A. de Gouw^{1,2}, and Jose L.
14 Jimenez^{1,2,+}

15

16 1. Department of Chemistry, University of Colorado, Boulder, Boulder, CO, USA

17 2. Cooperative Institute for Research in Environmental Sciences, Boulder, Colorado, USA

18 3. Chemical Sciences Division, NOAA Earth System Research Laboratory, Boulder, CO

19 4. National Centre for Atmospheric Sciences, School of Earth and Environmental Sciences, University of Manchester, Manchester, UK

20 5. Centre of Atmospheric Science, School of Earth and Environmental Sciences, University of Manchester, Manchester, UK

21 6. Department of Chemistry, University of California, Irvine, Irvine, CA, USA

22 7. Center for Aerosol and Cloud Chemistry, Aerodyne Research Inc., Billerica, MA, USA

23 8. Department of Environmental Health Engineering, Johns Hopkins University, Baltimore, MD, USA

24 9. NASA Langley Research Center, Hampton, Virginia, USA

25 10. Wolfson Atmospheric Chemistry Laboratories, Department of Chemistry, University of York, York, UK

26 11. Atmospheric Chemistry Observations and Modeling Laboratory, National Center for Atmospheric Research, Boulder, CO, USA

27 12. Institute of Arctic and Alpine Research, University of Colorado, Boulder, CO, USA

28 13. Atmospheric Chemistry and Dynamic Laboratory, NASA Goddard Space Flight Center, Greenbelt, MD, USA

29 14. Department of Chemistry, Université de Montréal, Montréal, QC, Canada

30 15. Department of Mechanical Engineering, University of Colorado, Boulder, CO, USA

31 16. Laboratoires d'Aréologie, Université de Toulouse, CNRS, UPS, Toulouse, France

32 17. National Centre for Atmospheric Sciences, Department of Chemistry, University of York, York, UK

33 18. State Key Joint Laboratory of Environmental Simulation and Pollution Control, College of Environmental Sciences and Engineering, Peking

34 University, Beijing, China

35 19. School of Earth and Atmospheric Sciences, Georgia Institute of Technology, Atlanta, Georgia, USA

36 20. Laboratory for Atmospheric Research, Department of Civil and Environmental Engineering, Washington State University, Pullman, WA,

37 USA

38 21. Universities Space Research Association, GESTAR, Columbia, MD, USA

39 22. Department of Atmospheric Science, Colorado State University, Fort Collins, CO, USA

40 23. Department of Earth and Atmospheric Science, University of Houston, Houston, TX, USA

41 24. Centre for Ocean and Atmospheric Sciences, School of Environmental Sciences, University of East Anglia, Norwich, UK

42 25. Institute for Environmental and Climate Research, Jinan University, Guangzhou, China

43 26. Air Quality Research Division, Environment and Climate Change Canada, Toronto, Ontario, Canada

44 27. Joint Center for Earth Systems Technology, University of Maryland, Baltimore County, Baltimore, MD, USA

45 28. Ministry of Education Key Laboratory for Earth System Modeling, Department of Earth System Science, Tsinghua University, Beijing, China

46 *Now at Center for Aerosol and Cloud Chemistry, Aerodyne Research Inc., Billerica, MA, USA

47 **Now at State Key Laboratory at Organic Geochemistry, Guangzhou Institute of Geochemistry, Chinese Academy of Sciences, Guangzhou,

48 China

49 ***Now at Colorado Department of Public Health and Environment, Denver, CO, USA

50 ****Now at Forschungszentrum Juelich GmbH, Juelich, Germany

51 *****Has retired and worked on this manuscript as an unaffiliated co-author.

52 *****Now at Scientific Aviation, Boulder, CO, USA

53 *****Now at Air Quality Research Center, University of California, Davis, CA, USA

54

55

56 +Corresponding author: Benjamin A. Nault (bnault@aerodyne.com), Jose L. Jimenez

57 (jose.jimenez@colorado.edu)

58

59 **Abstract**

60 Anthropogenic secondary organic aerosol (ASOA), formed from anthropogenic emissions of
61 organic compounds, constitutes a substantial fraction of the mass of submicron aerosol in
62 populated areas around the world and contributes to poor air quality and premature mortality.
63 However, the precursor sources of ASOA are poorly understood, and there are large uncertainties
64 in the health benefits that might accrue from reducing anthropogenic organic emissions. We
65 show that the production of ASOA in 11 urban areas on three continents is strongly correlated
66 with the reactivity of specific anthropogenic volatile organic compounds. The differences in
67 ASOA production across different cities can be explained by differences in the emissions of
68 aromatics and intermediate- and semi-volatile organic compounds, indicating the importance of
69 controlling these ASOA precursors. With an improved modeling representation of ASOA driven
70 by the observations, we attribute 340,000 $PM_{2.5}$ premature deaths per year to ASOA, which is
71 over an order of magnitude higher than prior studies. A sensitivity case with a more recently
72 proposed model for attributing mortality to $PM_{2.5}$ (the Global Exposure Mortality Model) results
73 in up to 900,000 deaths. A limitation of this study is the extrapolation from cities with detailed
74 studies and regions where detailed emission inventories are available to other regions where
75 uncertainties in emissions are larger. In addition to further development of institutional air
76 quality management infrastructure, comprehensive air quality campaigns in the countries in
77 South and Central America, Africa, South Asia, and the Middle East are needed for further
78 progress in this area.

79 **1. Introduction**

80 Poor air quality is one of the leading causes of premature mortality worldwide (Cohen et
81 al., 2017; Landrigan et al., 2018). Roughly 95% of the world's population live in areas where
82 $PM_{2.5}$ (fine particulate matter with diameter smaller than 2.5 μm) exceeds the World Health
83 Organization's 10 $\mu g m^{-3}$ annual average guideline (Shaddick et al., 2018). This is especially true
84 for urban areas, where high population density is co-located with increased emissions of $PM_{2.5}$
85 and its gas-phase precursors from human activities. It is estimated that $PM_{2.5}$ leads to 3 to 4
86 million premature deaths per year, higher than the deaths associated with other air pollutants
87 (Cohen et al., 2017). More recent analysis using concentration-response relationships derived
88 from studies of populations exposure to high levels of ambient $PM_{2.5}$ suggest the global
89 premature death burden could be up to twice this value (Burnett et al., 2018).

90 The main method to estimate premature mortality with $PM_{2.5}$ is to use measured $PM_{2.5}$
91 from ground observations along with derived $PM_{2.5}$ from satellites to fill in missing ground-based
92 observations (van Donkelaar et al., 2015, 2016). To go from total $PM_{2.5}$ to species-dependent and
93 even sector-dependent associated premature mortality from $PM_{2.5}$, chemical transport models
94 (CTMs) are used to predict the fractional contribution of species and/or sector (e.g., Lelieveld et
95 al., 2015; van Donkelaar et al., 2015, 2016; Silva et al., 2016). However, though CTMs may get
96 total $PM_{2.5}$ or even total species, e.g., organic aerosol (OA), correct, the model may be getting the
97 values right for the wrong reason (e.g., de Gouw and Jimenez, 2009; Woody et al., 2016; Murphy
98 et al., 2017; Baker et al., 2018; Hodzic et al., 2020). This is especially important for OA in urban
99 areas, where models have a longstanding issue under predicting secondary OA (SOA) with some
100 instances of over predicting primary OA (POA) (de Gouw and Jimenez, 2009; Dzepina et al.,

101 2009; Hodzic et al., 2010b; Woody et al., 2016; Zhao et al., 2016a; Janssen et al., 2017; Jathar et
102 al., 2017). Further, this bias has even been observed for highly aged aerosols in remote regions
103 (Hodzic et al., 2020). As has been found in prior studies for urban areas (e.g., Zhang et al., 2007;
104 Kondo et al., 2008; Jimenez et al., 2009; DeCarlo et al., 2010; Hayes et al., 2013; Freney et al.,
105 2014; Hu et al., 2016; Nault et al., 2018; Schroder et al., 2018) and highlighted here (Fig. 1), a
106 substantial fraction of the observed submicron PM is OA, and a substantial fraction of the OA is
107 composed of SOA (approximately a factor of 2 to 3 higher than POA). Thus, to better understand
108 the sources and apportionment of PM_{2.5} that contributes to premature mortality, CTMs must
109 improve their prediction of SOA versus POA, as the sources of SOA precursors and POA can be
110 different.

111 However, understanding the gas-phase precursors of photochemically-produced
112 anthropogenic SOA (ASOA, defined as the photochemically-produced SOA formed from the
113 photooxidation of anthropogenic volatile organic compounds (AVOC) (de Gouw et al., 2005;
114 DeCarlo et al., 2010)) quantitatively is challenging (Hallquist et al., 2009). Note, for the rest of
115 the paper, unless explicitly stated otherwise, ASOA refers to SOA produced from the
116 photooxidation of AVOCs, as there are potentially other relevant paths for the production of SOA
117 in urban environments (e.g., Petit et al., 2014; Kodros et al., 2018, 2020; Stavroulas et al., 2019).
118 Though the enhancement of ASOA is largest in large cities, these precursors and production of
119 ASOA should be important in any location impacted by anthropogenic emissions (e.g., Fig. 1).
120 ASOA comprises a wide range of condensable products generated by numerous chemical
121 reactions involving AVOC precursors (Hallquist et al., 2009; Hayes et al., 2015; Shrivastava et
122 al., 2017). The number of AVOC precursors, as well as the role of “non-traditional” AVOC

123 precursors, along with the condensable products and chemical reactions, compound to lead to
124 differences in the observed versus predicted ASOA for various urban environments (e.g., de
125 Gouw and Jimenez, 2009; Dzepina et al., 2009; Hodzic et al., 2010b; Woody et al., 2016; Janssen
126 et al., 2017; Jathar et al., 2017; McDonald et al., 2018). One solution to improve the prediction in
127 CTMs is to use a simplified model, where lumped ASOA precursors react, non-reversibly, at a
128 given rate constant, to produce ASOA (Hodzic and Jimenez, 2011; Hayes et al., 2015; Pai et al.,
129 2020). This simplified model has been found to reproduce the observed ASOA from some urban
130 areas (Hodzic and Jimenez, 2011; Hayes et al., 2015) but issues in other urban areas (Pai et al.,
131 2020). This may stem from the simplified model being parameterized to two urban areas (Hodzic
132 and Jimenez, 2011; Hayes et al., 2015). These inconsistencies impact the model predicted
133 fractional contribution of ASOA to total $PM_{2.5}$ and thus the ability to understand the source
134 attribution to $PM_{2.5}$ and premature deaths.

135 The main categories of gas-phase precursors that dominate ASOA have been the subject
136 of intensive research. The debate on what dominates can in turn impact the understanding of
137 what precursors to regulate to reduce ASOA, to improve air quality, and to reduce premature
138 mortality associated with ASOA. Transportation-related emissions (e.g., tailpipe, evaporation,
139 refueling) were assumed to be the major precursors of ASOA, which was supported by field
140 studies (Parrish et al., 2009; Gentner et al., 2012; Warneke et al., 2012; Pollack et al., 2013). Yet,
141 budget closure of observed ASOA mass concentrations could not be achieved with
142 transportation-related VOCs (Ensberg et al., 2014). The contribution of urban-emitted biogenic
143 precursors to SOA in urban areas is typically small. Biogenic SOA (BSOA) in urban areas
144 typically results from advection of regional background concentrations rather than processing of

145 locally emitted biogenic VOCs (e.g., Hodzic et al., 2009, 2010a; Hayes et al., 2013; Janssen et
146 al., 2017). BSOA is thought to dominate globally (Hallquist et al., 2009), but as shown in Fig. 1,
147 the contribution of BSOA (1% to 20%) to urban concentrations, while often substantial, is
148 typically smaller than that of ASOA (17% to 39%) (see Sect. S3.1).

149 Many of these prior studies generally investigated AVOC with high volatility, where
150 volatility here is defined as the saturation concentration, C^* , in $\mu\text{g m}^{-3}$ (de Gouw et al., 2005;
151 Volkamer et al., 2006; Dzepina et al., 2009; Freney et al., 2014; Woody et al., 2016). More recent
152 studies have identified lower volatility compounds in transportation-related emissions (e.g., Zhao
153 et al., 2014, 2016b; Lu et al., 2018). These compounds have been broadly identified as
154 intermediate-volatile organic compounds (IVOCs) and semi-volatile organic compounds
155 (SVOCs). IVOCs have a C^* generally of 10^3 to $10^6 \mu\text{g m}^{-3}$ while SVOCs have a C^* generally of
156 1 to $10^2 \mu\text{g m}^{-3}$. Due to their lower volatility and functional groups, these classes of compounds
157 generally form ASOA more efficiently than traditional, higher volatile AVOCs; however,
158 S/IVOCs have also been more difficult to measure (e.g., Zhao et al., 2014; Pagonis et al., 2017;
159 Deming et al., 2018). IVOCs generally have been the more difficult of the two classes to measure
160 and identify as these compounds cannot be collected onto filters to be sampled off-line (Lu et al.,
161 2018) and generally show up as unresolved complex mixture for in-situ measurements using
162 gas-chromatography (GC) (Zhao et al., 2014). SVOCs, on the other hand, can be more readily
163 collected onto filters and sampled off-line due to their lower volatility (Lu et al., 2018). Another
164 potential issue has been an under-estimation of the S/IVOC aerosol production, as well as an
165 under-estimation in the contribution of photochemically produced S/IVOC from photooxidized
166 “traditional” VOCs, due to partitioning of these low volatile compounds to chamber walls and

167 tubing (Krechmer et al., 2016; Ye et al., 2016; Liu et al., 2019). Accounting for this
168 under-estimation increases the predicted ASOA (Ma et al., 2017). The inclusion of these classes
169 of compounds have led to improvement in some urban SOA budget closure; however, many
170 studies still have indicated a general short-fall in ASOA budget even when including these
171 compounds from transportation-related emissions. (Dzepina et al., 2009; Tsimpidi et al., 2010;
172 Hayes et al., 2015; Cappa et al., 2016; Ma et al., 2017; McDonald et al., 2018).

173 Recent studies have indicated that emissions from volatile chemical products (VCPs),
174 defined as pesticides, coatings, inks, adhesives, personal care products, and cleaning agents
175 (McDonald et al., 2018), as well as cooking emissions (Hayes et al., 2015), asphalt emissions
176 (Khare et al., 2020), and solid fuel emissions from residential wood burning and/or cookstoves
177 (e.g., Hu et al., 2013, 2020; Schroder et al., 2018), are important. While total amounts of ASOA
178 precursors released in cities have dramatically declined (largely due to three-way catalytic
179 converters in cars (Warneke et al., 2012; Pollack et al., 2013; Zhao et al., 2017; Khare and
180 Gentner, 2018)), VCPs have not declined as quickly (Khare and Gentner, 2018; McDonald et al.,
181 2018). Besides a few cities in the US (Coggon et al., 2018; Khare and Gentner, 2018; McDonald
182 et al., 2018), extensive VCP emission quantification has not yet been published.

183 Due to the uncertainty on the emissions of ASOA precursors and on the amount of
184 ASOA formed from them, the number of premature deaths associated with urban organic
185 emissions is largely unknown. Since numerous studies have shown the importance of VCPs and
186 other non-traditional VOC emission sources, efforts have been made to try to improve the
187 representation and emissions of VCPs (Seltzer et al., 2021), which can reduce the uncertainty in
188 ASOA precursors and the associated premature deaths estimations. Currently, most studies have

189 not treated ASOA explicitly (e.g., Lelieveld et al., 2015; Silva et al., 2016; Ridley et al., 2018) in
190 source apportionment calculations of the premature deaths associated with long-term exposure of
191 $PM_{2.5}$. Most models represented total OA as non-volatile POA and “traditional” ASOA
192 precursors (transportation-based VOCs), which largely under-predict ASOA (Ensberg et al.,
193 2014; Hayes et al., 2015; Nault et al., 2018; Schroder et al., 2018) while over-predicting POA
194 (e.g., Hodzic et al., 2010b; Zhao et al., 2016a; Jathar et al., 2017). This does not reflect the
195 current understanding that POA is volatile and contributes to ASOA mass concentration (e.g.,
196 Grieshop et al., 2009; Lu et al., 2018). Though the models are estimating total OA correctly
197 (Ridley et al., 2018; Hodzic et al., 2020; Pai et al., 2020), the attribution of premature deaths to
198 POA instead of SOA formed from “traditional” and “non-traditional” sources, including IVOCs
199 from both sources, could lead to regulations that may not target the emissions that would reduce
200 OA in urban areas. As PM_1 and SOA mass are highest in urban areas (Fig. 1), also shown in
201 Jimenez et al. (2009), it is necessary to quantify the amount and identify the sources of ASOA to
202 target future emission standards that will optimally improve air quality and the associated health
203 impacts. As these emissions are from human activities, they will contribute to SOA mass outside
204 urban regions and to potential health impacts outside urban regions as well. Though there are
205 potentially other important exposure pathways to PM that may increase premature mortality,
206 such as exposure to solid-fuel emissions indoors (e.g., Kodros et al., 2018), the focus of this
207 paper is on exposure to outdoor ASOA and its associated impacts to premature mortality.

208 Here, we investigate the factors that control ASOA using 11 major urban, including
209 megacities, field studies (Fig. 1 and Table 1). The empirical relationships and numerical models
210 are then used to quantify the attribution of premature mortality to ASOA around the world, using

211 the observations to improve the modeled representation of ASOA. The results provide insight
212 into the importance of ASOA to global premature mortality due to $PM_{2.5}$ and further
213 understanding of the precursors and sources of ASOA in urban regions.

214

215 **2. Methods**

216 Here, we introduce the ambient observations from various campaigns used to constrain
217 ASOA production (Sect. 2.1), description of the simplified model used in CTMs to better predict
218 ASOA (Sect. 2.2), and description of how premature mortality was estimated for this study (Sect.
219 2.3). In the SI, the following can be found: description of the emissions used to calculate the
220 ASOA budget for five different locations (Sect. S1), description of how the ASOA budget was
221 calculated for the five different locations (Sect. S2), description of the CTM (GEOS-Chem) used
222 in this study (Sect. S3 - S4), and error analysis for the observations (Sect. S5).

223

224 **2.1 Ambient Observations**

225 For values not previously reported in the literature (Table S4), observations taken
226 between 11:00 – 16:00 local time were used to determine the slopes of SOA versus
227 formaldehyde (HCHO) (Fig. S1), peroxy acetyl nitrate (PAN) (Fig. S2), and O_x ($O_x = O_3 + NO_2$)
228 (Fig. S3). For CalNex, there was an approximate 48% difference between the two HCHO
229 measurements (Fig. S4). Therefore, the average between the two measurements were used in this
230 study, similar to what has been done in other studies for other gas-phase species (Bertram et al.,
231 2007). All linear fits, unless otherwise noted, use the orthogonal distance regression fitting
232 method (ODR).

233 For values in Table S4 through Table S8 not previously reported in the literature, the
 234 following procedure was applied to determine the emissions ratios, similar to the methods of
 235 Nault et al. (2018). An OH exposure ($OH_{exp} = [OH] \times \Delta t$), which is also the photochemical age
 236 (PA), was estimated by using the ratio of NO_x/NO_y (Eq. 1) or the ratio of
 237 m+p-xylene/ethylbenzene (Eq. 2). For the m+p-xylene/ethylbenzene, the emission ratio
 238 (Table S5) was determined by determining the average ratio during minimal photochemistry,
 239 similar to prior studies (de Gouw et al., 2017). This was done for only one study, TexAQS 2000.
 240 This method could be applied in that case as it was a ground campaign that operated both day
 241 and night; therefore, a ratio at night could be determined when there was minimal loss of both
 242 VOCs. The average emission ratio for the other VOCs was determined using Eq. 3 after the
 243 OH_{exp} was calculated in Eq. 1 or Eq. 2. The rate constants used for determining OH_{exp} and
 244 emission ratios are found in Table S12.

$$245 \quad OH_{exp} = [OH] \times t = \ln \left(\frac{\left(\frac{[NO_x]}{[NO_y]} \right)}{k_{OH+NO_2}} \right) \quad \text{Eq. 1}$$

$$246 \quad OH_{exp} = [OH] \times t = - \frac{1}{k_{m+p-xylene} - k_{ethylbenzene}} \times \ln \left(\frac{[m+p-xylene]_t}{[ethylbenzene]_t} - \frac{[m+p-xylene]_0}{[ethylbenzene]_0} \right) \quad \text{Eq. 2}$$

$$248 \quad \frac{[VOC(i)]}{[CO]}(0) = - \frac{[VOC(i)]}{[CO]}(t) \times \left(1 - \frac{1}{\exp(-k_i \times [OH]_{exp} \times t)} \right) \times k_i + \frac{[VOC(i)]}{[CO]}(t) \times k_i \quad \text{Eq. 3}$$

251 **2.2 Updates to the SIMPLE Model**

252 With the combination of the new dataset, which expands across urban areas on three
253 continents, the SIMPLE parameterization for ASOA (Hodzic and Jimenez, 2011) is updated in
254 the standard GEOS-Chem model to reproduce observed ASOA in Fig. 2a. The parameterization
255 operates as represented by Eq. 4.



257 SOAP represents the lumped precursors of ASOA, k is the reaction rate coefficient with OH
258 ($1.25 \times 10^{-11} \text{ cm}^3 \text{ molecules}^{-1} \text{ s}^{-1}$), and $[\text{OH}]$ is the OH concentration in molecules cm^{-3} . This rate
259 constant is also consistent with observed ASOA formation time scale of ~ 1 day that has been
260 observed across numerous studies (e.g., de Gouw et al., 2005; DeCarlo et al., 2010; Hayes et al.,
261 2013; Nault et al., 2018; Schroder et al., 2018).

262 SOAP emissions were calculated based on the relationship between $\Delta\text{SOA}/\Delta\text{CO}$ and
263 $R_{\text{aromatics}}/\Delta\text{CO}$ in Fig. 2a. First, we calculated $R_{\text{aromatics}}/\Delta\text{CO}$ (Eq. 5) for each grid cell and time step
264 as follows:

$$265 \quad \frac{R_{\text{aromatics}}}{\Delta\text{CO}} = \frac{E_{\text{B}} \times k_{\text{B}} + E_{\text{T}} \times k_{\text{T}} + E_{\text{X}} \times k_{\text{X}}}{E_{\text{CO}}} \quad \text{Eq. 5}$$

266 Where E and k stand for the emission rate and reaction rate coefficient with OH, respectively, for
267 benzene (B), toluene (T), and xylenes (X). Ethylbenzene was not included in this calculation
268 because its emission was not available in HTAPv2 emission inventory. However, ethylbenzene
269 contributed a minor fraction of the mixing ratio ($\sim 7\%$, Table S5) and reactivity ($\sim 6\%$) of the
270 total BTEX across the campaigns. Reaction rate constants used in this study were 1.22×10^{-12} ,
271 5.63×10^{-12} , and $1.72 \times 10^{-11} \text{ cm}^3 \text{ molec.}^{-1} \text{ s}^{-1}$ for benzene, toluene, and xylene, respectively
272 (Atkinson and Arey, 2003; Atkinson et al., 2006). The $R_{\text{aromatics}}/\Delta\text{CO}$ allows a dynamic

273 calculation of the $E(\text{VOC})/E(\text{CO}) = \text{SOA}/\Delta\text{CO}$. Hodzic and Jimenez (2011) and Hayes et al.
 274 (2015) used a constant value of 0.069 g g^{-1} , which worked well for the two cities investigated,
 275 but not for the expanded dataset studied here. Thus, both the aromatic emissions and CO
 276 emissions are used in this study to better represent the variable emissions of ASOA precursors
 277 (Fig. S5).

278 Second, $E_{\text{SOAP}}/E_{\text{CO}}$ can be obtained from the result of Eq. 6, using slope and intercept in
 279 Fig. 2a, with a correction factor (F) to consider additional SOA production after 0.5 PA
 280 equivalent days, since Fig. 2a shows the comparison at 0.5 PA equivalent days.

$$281 \quad \frac{E_{\text{SOAP}}}{E_{\text{CO}}} = \left(\text{Slope} \times \frac{R_{\text{Aromatics}}}{\Delta\text{CO}} + \text{Intercept} \right) \times F \quad \text{Eq. 6}$$

282 Where slope is 24.8 and intercept is -1.7 from Fig. 2a. F (Eq. 7) can be calculated as follows:

$$283 \quad F = \frac{ASOA_{t=\infty}}{ASOA_{t=0.5d}} = \frac{SOAP_{t=0}}{SOAP_{t=0} \times (1 - \exp(-k \times \Delta t \times [\text{OH}])), \Delta t = 43200 \text{ s}} \quad \text{Eq. 7}$$

284 F was calculated as 1.8 by using $[\text{OH}] = 1.5 \times 10^6 \text{ molecules cm}^{-3}$, which was used in the
 285 definition of 0.5 PA equivalent days for Fig. 2a.

286 Finally, E_{SOAP} can be computed by multiplying CO emissions (E_{CO}) for every grid point
 287 and time step in GEOS-Chem by the $E_{\text{SOAP}}/E_{\text{CO}}$ ratio.

288

289 **2.3 Estimation of Premature Mortality Attribution**

290 Premature deaths were calculated for five disease categories: ischemic heart disease
 291 (IHD), stroke, chronic obstructive pulmonary disease (COPD), acute lower respiratory illness
 292 (ALRI), and lung cancer (LC). We calculated premature mortality for the population aged more
 293 than 30 years, using Eq. 8.

294
$$Premature\ Death = Pop \times y_0 \times \frac{RR - 1}{RR}$$
 Eq. 8

295 Mortality rate, y_0 , varies according to the particular disease category and geographic region,
 296 which is available from Global Burden of Disease (GBD) Study 2015 database (IHME, 2016).
 297 Population (Pop) was obtained from Columbia University Center for International Earth Science
 298 Information Network (CIESIN) for 2010 (CIESIN, 2017). Relative risk, RR, can be calculated as
 299 shown in Eq. 9.

300
$$RR = 1 + \alpha \times \left(1 - \exp\left(\beta \times \left(PM_{2.5} - PM_{2.5,Threshold}\right)^\rho\right)\right)$$
 Eq. 9

301 α , β , and ρ values depend on disease category and are calculated from Burnett et al. (2014) (see
 302 Table S14 and associated file). If the $PM_{2.5}$ concentrations are below the $PM_{2.5}$ threshold value
 303 (Table S14), premature deaths were computed as zero. However, there could be some health
 304 impacts at concentrations below the $PM_{2.5}$ threshold values (Krewski et al., 2009); following the
 305 methods of the GBD studies, these can be viewed as lower bounds on estimates of premature
 306 deaths.

307 We performed an additional sensitivity analysis using the Global Exposure Mortality
 308 Model (GEMM) (Burnett et al., 2018). For the GEMM analysis, we also used age stratified
 309 population data from GWPv3. Premature death is calculated the same as shown in Eq. 8;
 310 however, the relative risk differs. For the GEMM model, the relative risk can be calculated as
 311 shown in Eq. 10.

312
$$RR = \exp(\theta \times \lambda) \text{ with } \lambda = \frac{\log\left(1 + \frac{z}{\alpha}\right)}{\left(1 + \exp\left(\frac{(\hat{\mu} - z)}{\pi}\right)\right)}$$
 Eq. 10

313 Here $z = \max(0, PM_{2.5} - PM_{2.5, Threshold})$; θ , π , $\hat{\mu}$, α , and $PM_{2.5, Threshold}$ depends on disease category and
314 are from Burnett et al. (2018). Similar to the Eq. 9, if the concentrations are below the threshold
315 ($2.4 \mu g m^{-3}$, Burnett et al. (2018)), then premature deaths are computed as zero; however, the
316 GEMM has a lower threshold than the GBD method.

317 For GBD, we do not consider age-specific mortality rates or risks. For GEMM, we
318 calculate age-specific health impacts with age-specific parameters in the exposure response
319 function (Table S15). We combine the age-specific results of the exposure-response function
320 with age distributed population data from GPW (CIESIN, 2017) and a national mortality rate
321 across all ages to assess age-specific mortality.

322 We calculated total premature deaths using annual average total $PM_{2.5}$ concentrations
323 derived from satellite-based estimates at the resolution of $0.1^\circ \times 0.1^\circ$ from van Donkelaar et al.
324 (2016) . Application of the remote-sensing based $PM_{2.5}$ at the $0.1^\circ \times 0.1^\circ$ resolution rather than
325 direct use of the GEOS-Chem model concentrations at the $2^\circ \times 2.5^\circ$ resolution helps reduce
326 uncertainties in the quantification of $PM_{2.5}$ exposure inherent in coarser estimates (Punger and
327 West, 2013). We also calculated deaths by subtracting from this amount the total annual average
328 ASOA concentrations derived from GEOS-Chem (Fig. S11). To reduce uncertainties related to
329 spatial gradients and total concentration magnitudes in our GEOS-Chem simulations of $PM_{2.5}$,
330 our modeled ASOA was calculated as the fraction of ASOA to total $PM_{2.5}$ in GEOS-Chem,
331 multiplied by the satellite-based $PM_{2.5}$ concentrations (Eq. 11).

$$332 \quad ASOA_{sat} = (ASOA_{mod} / PM_{2.5, mod}) \times PM_{2.5, sat} \quad \text{Eq. 11}$$

333 Finally, this process for estimating $PM_{2.5}$ health impacts considers only $PM_{2.5}$ mass concentration
334 and does not distinguish toxicity by composition, consistent with the current US EPA position
335 expressed in Sacks et al. (2019).

336

337 **3. Observations of ASOA Production across Three Continents**

338 **3.1 Observational Constraints of ASOA Production across Three Continents**

339 Measurements during intensive field campaigns in large urban areas better constrain
340 concentrations and atmospheric formation of ASOA because the scale of ASOA enhancement is
341 large compared to SOA from a regional background. Generally, ASOA increased with the
342 amount of urban precursor VOCs and with atmospheric PA (de Gouw et al., 2005; de Gouw and
343 Jimenez, 2009; DeCarlo et al., 2010; Hayes et al., 2013; Nault et al., 2018; Schroder et al., 2018;
344 Shah et al., 2018). In addition, ASOA correlates strongly with gas-phase secondary
345 photochemical species, including O_x , HCHO, and PAN (Herndon et al., 2008; Wood et al., 2010;
346 Hayes et al., 2013; Zhang et al., 2015; Nault et al., 2018; Liao et al., 2019) (Table S4; Fig. S1 to
347 Fig. S3), which are indicators of photochemical processing of emissions.

348 However, as initially discussed by Nault et al. (2018) and shown in Fig. 3, there is large
349 variability in these various metrics across the urban areas evaluated here. To the best of the
350 authors' knowledge, this variability has not been explored and its physical meaning has not been
351 interpreted. As shown in Fig. 3, though, the trends in $\Delta SOA/\Delta CO$ are similar to the trends in the
352 slopes of SOA versus O_x , PAN, or HCHO. For example, Seoul is the highest for nearly all
353 metrics, and is approximately a factor of 6 higher than the urban area, Houston, that generally

354 showed the lowest photochemical metrics. This suggests that the variability is related to a
355 physical factor, including emissions and chemistry.

356 The VOC concentration, together with how quickly the emitted VOCs react ($\sum k_i \times [\text{VOC}]_i$,
357 i.e., the hydroxyl radical, or OH, reactivity of VOCs), where k is the OH rate coefficient for each
358 VOC, are a determining parameter for ASOA formation over urban spatial scales (Eq. 12).
359 ASOA formation is normalized here to the excess CO mixing ratio (ΔCO) to account for the
360 effects of meteorology, dilution, and non-urban background levels, and allow for easier
361 comparison between different studies:

$$362 \quad \frac{\Delta \text{ASOA}}{\Delta \text{CO}} \propto [\text{OH}] \times \Delta t \times \left(\sum_i k_i \times \left[\frac{\text{VOC}}{\text{CO}} \right]_i \times Y_i \right) \quad \text{Eq. 12}$$

363 where Y is the aerosol yield for each compound (mass of SOA formed per unit mass of precursor
364 reacted), and $[\text{OH}] \times \Delta t$ is the PA.

365 BTEX are one group of known ASOA precursors (Gentner et al., 2012; Hayes et al.,
366 2013), and their emission ratio (to CO) was determined for all campaigns (Table S5). BTEX can
367 thus provide insight into ASOA production. Fig. 2a shows that the variation in ASOA (at PA =
368 0.5 equivalent days) is highly correlated with the emission reactivity ratio of BTEX (R_{BTEX} ,
369 $\sum_i [\text{VOC}/\text{CO}]_i$) across all the studies. However, BTEX alone cannot account for much of the
370 ASOA formation (see budget closure discussion below), and instead, BTEX may be better
371 thought of as both partial contributors and also as indicators for the co-emission of other
372 (unmeasured) organic precursors that are also efficient at forming ASOA.

373 O_x , PAN, and HCHO are produced from the oxidation of a much wider set of VOC
374 precursors (including small alkenes, which do not appreciably produce SOA when oxidized).

375 These alkenes have similar reaction rate constants with OH as the most reactive BTEX
376 compounds (Table S12); however, their emissions and concentration can be higher than BTEX
377 (Table S7). Thus, alkenes would dominate R_{Total} , leading to O_x , HCHO, and PAN being produced
378 more rapidly than ASOA (Fig. 2b–d). When R_{BTEX} becomes more important for R_{Total} , the emitted
379 VOCs are more efficient in producing ASOA. Thus, the ratio of ASOA to gas-phase
380 photochemical products shows a strong correlation with $R_{\text{BTEX}}/R_{\text{Total}}$ (Fig. 2b–d).

381 An important aspect of this study is that most of these observations occurred during
382 spring and summer, when solid fuel emissions are expected to be lower (e.g., Chafe et al., 2015;
383 Lam et al., 2017; Hu et al., 2020). Further, the most important observations used here are during
384 the afternoon, investigating specifically the photochemically produced ASOA. These results here
385 might partially miss any ASOA produced through nighttime aqueous chemistry or oxidation by
386 nitrate radical (Kodros et al., 2020). However, two of the studies included in our analysis,
387 Chinese Outflow (CAPTAIN, 2011) and New York City (WINTER, 2015), occurred in late
388 winter/early spring, when solid fuel emissions were important (Hu et al., 2013; Schroder et al.,
389 2018). We find that these observations lie within the uncertainty in the slope between ASOA and
390 R_{BTEX} (Fig. 2a). Their photochemically produced ASOA observed under strong impact from solid
391 fuel emissions shows similar behavior as the ASOA observed during spring and summer time.
392 Thus, given the limited datasets currently available, photochemically produced ASOA is
393 expected to follow the relationship shown in Fig. 2a and is expected to also follow this
394 relationship for regions impacted by solid fuel burning. Future comprehensive studies in regions
395 strongly impacted by solid fuel burning are needed to further investigate photochemical ASOA
396 production under those conditions.

397

398 **3.2 Budget Closure of ASOA for 4 Urban Areas on 3 Continents Indicates Reasonable** 399 **Understanding of ASOA Sources**

400 To investigate the correlation between ASOA and R_{BTEX} , a box model using the emission
401 ratios from BTEX (Table S5), other aromatics (Table S8), IVOCs (Sect. S1), and SVOCs (Sect.
402 S1) was run for five urban areas: New York City, 2002, Los Angeles, Beijing, London, and New
403 York City, 2015 (see Sect. S1 and S3 for more information). The differences in the results shown
404 in Fig. 4 are due to differences in the emissions for each city. We show that BTEX alone cannot
405 explain the observed ASOA budget for urban areas around the world. Fig. 4a shows that
406 approximately $25 \pm 6\%$ of the observed ASOA originates from the photooxidation of BTEX.
407 BTEX only explaining 25% of the observed ASOA is similar to prior studies that have done
408 budget analysis of precursor gases and observed SOA (e.g., Dzepina et al., 2009; Ensberg et al.,
409 2014; Hayes et al., 2015; Ma et al., 2017; Nault et al., 2018). Therefore, other precursors must
410 account for most of the ASOA produced.

411 Because alkanes, alkenes, and oxygenated compounds with carbon numbers less than 6
412 are not significant ASOA precursors, we focus on emissions and sources of BTEX, other
413 mono-aromatics, IVOCs, and SVOCs. These three classes of VOCs, aromatics, IVOCs, and
414 SVOCs, have been suggested to be significant ASOA precursors in urban atmospheres
415 (Robinson et al., 2007; Hayes et al., 2015; Ma et al., 2017; McDonald et al., 2018; Nault et al.,
416 2018; Schroder et al., 2018; Shah et al., 2018), originating from both fossil fuel and VCP
417 emissions.

418 Using the best available emission inventories from cities on three continents
419 (EMEP/EEA, 2016; McDonald et al., 2018; Li et al., 2019) and observations, we quantify the
420 emissions of BTEX, other mono-aromatics, IVOCs, and SVOCs for both fossil fuel (e.g.,
421 gasoline, diesel, kerosene, etc.), VCPs (e.g., coatings, inks, adhesives, personal care products,
422 and cleaning agents), and cooking sources (Fig. 5). This builds off the work of McDonald et al.
423 (2018) for urban regions on three different continents.

424 Note, the emissions investigated here ignore any oxygenated VOC emissions not
425 associated with IVOCs and SVOCs due to the challenge in estimating the emission ratios for
426 these compounds (de Gouw et al., 2018). Further, SVOC emission ratios are estimated from the
427 average POA observed by the AMS during the specific campaign and scaled by profiles in
428 literature for a given average temperature and average OA (Robinson et al., 2007; Worton et al.,
429 2014; Lu et al., 2018). As most of the campaigns had an average OA between 1 and 10 $\mu\text{g m}^{-3}$
430 and temperature of ~ 298 K, this led to the majority of the estimated emitted SVOC gases in the
431 highest SVOC bin. However, as discussed later, this does not lead to SVOCs dominating the
432 predicted ASOA due to taking into account the fragmentation and overall yield from the
433 photooxidation of SVOC to ASOA.

434 Combining these inventories and observations for the various locations provide the
435 following insights about the potential ASOA precursors not easily measured or quantified in
436 urban environments (e.g., Zhao et al., 2014; Lu et al., 2018): (1) aromatics from fossil fuel
437 accounts for 14-40% (mean 22%) of the total BTEX and IVOC emissions for the five urban
438 areas investigated in-depth (Fig. 5), agreeing with prior studies that have shown that the observed
439 ASOA cannot be reconciled by the observations or emission inventory of aromatics from fossil

440 fuels (e.g., Ensberg et al., 2014; Hayes et al., 2015). (2) BTEX from both fossil fuels and VCPs
441 account for 25-95% (mean 43%) of BTEX and IVOC emissions (Fig. 5). China has the lowest
442 contribution of IVOCs, potentially due to differences in chemical make-up of the solvents used
443 daily (Li et al., 2019), but more research is needed to investigate the differences in IVOCs:BTEX
444 from Beijing versus US and UK emission inventories. Nonetheless, this shows the importance of
445 IVOCs for both emissions and ASOA precursors. (3) IVOCs are generally equal to, if not greater
446 than, the emissions of BTEX in 4 of the 5 urban areas investigated here (Fig. 5). (4) Overall,
447 VCPs account for a large fraction of the BTEX and IVOC emissions for all five cities. (5)
448 Finally, SVOCs account for 27-88% (mean 53%) of VOCs generally considered ASOA
449 precursors (VOCs with volatility saturation concentrations $\leq 10^7 \mu\text{g m}^{-3}$) (Fig. S6). Beijing has
450 the highest contribution of SVOCs to ASOA precursors due to the use of solid fuels and cooking
451 emissions (Hu et al., 2016). Also, this indicates the large contribution of a class of VOCs
452 difficult to measure (Robinson et al., 2007) that are an important ASOA precursor (e.g., Hayes et
453 al., 2015), showing further emphasis should be placed in quantifying the emissions of this class
454 of compounds.

455 These results provide an ability to further investigate the mass balance of predicted and
456 observed ASOA for these urban locations (Fig. 4). The inclusion of IVOCs, other aromatics not
457 including BTEX, and SVOCs leads to the ability to explain, on average, $85\pm 12\%$ of the observed
458 ASOA for these urban locations around the world (Fig. 4a). Further, VCP contribution to ASOA
459 is important for all these urban locations, accounting for, on average, $37\pm 3\%$ of the observed
460 ASOA (Fig. 4b).

461 This bottom-up mass budget analysis provides important insights to further explain the
462 correlation observed in Fig. 2. First, IVOCs are generally co-emitted from similar sources as
463 BTEX for the urban areas investigated in-depth (Fig. 5). The oxidation of these co-emitted
464 species leads to the ASOA production observed across the urban areas around the world. Second,
465 S/IVOCs generally have similar rate constants as toluene and xylenes ($\geq 1 \times 10^{-11} \text{ cm}^3 \text{ molec.}^{-1} \text{ s}^{-1}$)
466 (Zhao et al., 2014, 2017), the compounds that contribute the most to R_{BTEX} , explaining the rapid
467 ASOA production that has been observed in various studies (de Gouw and Jimenez, 2009;
468 DeCarlo et al., 2010; Hayes et al., 2013; Hu et al., 2013, 2016; Nault et al., 2018; Schroder et al.,
469 2018) and correlation (Fig. 2). Finally, the contribution of VCPs and fossil fuel sources to ASOA
470 is similar across the cities, expanding upon and further supporting the conclusion of McDonald
471 et al. (2018) in the importance of identifying and understanding VCP emissions in order to
472 explain ASOA.

473 This investigation shows that the bottom-up calculated ASOA agrees with observed
474 top-down ASOA within 15%. As highlighted above, this ratio is explained by the co-emissions
475 of IVOCs with BTEX from traditional sources (diesel, gasoline, and other fossil fuel emissions)
476 and VCPs (Fig. 5) along with similar rate constants for these ASOA precursors (Table S12).
477 Thus, the $\text{ASOA}/R_{\text{BTEX}}$ ratio obtained from Fig. 2 results in accurate predictions of ASOA for the
478 urban areas evaluated here, and this value can be used to better estimate ASOA with chemical
479 transport models (Sect. 4).

480

481 **4. Improved Urban SIMPLE Model Using Multi-Cities to Constrain**

482 The SIMPLE model was originally designed and tested against the observations collected
483 around Mexico City (Hodzic and Jimenez, 2011). It was then tested against observations
484 collected in Los Angeles (Hayes et al., 2015; Ma et al., 2017). As both data sets have nearly
485 identical $\Delta\text{SOA}/\Delta\text{CO}$ and R_{BTEX} (Fig. 2 and Fig. 3), it is not surprising that the SIMPLE model
486 did well in predicting the observed $\Delta\text{SOA}/\Delta\text{CO}$ for these two urban regions with consistent
487 parameters. Though the SIMPLE model generally performed better than more explicit models, it
488 generally had lower skill in predicting the observed ASOA in urban regions outside of Mexico
489 City and Los Angeles (Shah et al., 2019; Pai et al., 2020).

490 This may stem from the original SIMPLE model with constant parameters missing the
491 ability to change the amount and reactivity of the emissions, which are different for the various
492 urban regions, versus the ASOA precursors being emitted proportionally to only CO (Hodzic and
493 Jimenez, 2011; Hayes et al., 2015). For example, in the HTAP emissions inventory, the CO
494 emissions for Seoul, Los Angeles, and Mexico City are all similar (Fig. S8); thus, the original
495 SIMPLE model would suggest similar $\Delta\text{SOA}/\Delta\text{CO}$ for all three urban locations. However, as
496 shown in Fig. 2 and Fig. 3, the $\Delta\text{SOA}/\Delta\text{CO}$ is different by nearly a factor of 2. The inclusion of
497 the emissions and reactivity, where R_{BTEX} for Seoul is approximately a factor of 2.5 higher than
498 Los Angeles and Seoul, into the improved SIMPLE model better accounts for the variability in
499 SOA production, as shown in Fig. 2. Thus, the inclusion and use of this improved SIMPLE
500 model refines the simplified representation of ASOA in chemical transport models and/or box
501 models.

502 The “improved” SIMPLE shows higher ASOA compared to the default VBS
503 GEOS-Chem (Fig. 6a,b). In areas strongly impacted by urban emissions (e.g., Europe, East Asia,

504 India, east and west coast US, and regions impacted by Santiago, Chile, Buenos Aires,
505 Argentina, Sao Paulo, Brazil, Durban and Cape Town, South Africa, and Melbourne and Sydney,
506 Australia), the “improved” SIMPLE model predicts up to $14 \mu\text{g m}^{-3}$ more ASOA, or ~30 to 60
507 times more ASOA than the default scheme (Fig. 6c,d). As shown in Fig. 1, during intensive
508 measurements, the ASOA composed 17-39% of PM_{10} , with an average contribution of ~25%. The
509 default ASOA scheme in GEOS-Chem greatly underestimates the fractional contribution of
510 ASOA to total $\text{PM}_{2.5}$ (<2%; Fig. 6e). The “improved” SIMPLE model greatly improves the
511 predicted fractional contribution, showing that ASOA in the urban regions ranges from 15-30%,
512 with an average of ~15% for the grid cells corresponding to the urban areas investigated here
513 (Fig. 6f). Thus, the “improved” SIMPLE predicts the fractional contribution of ASOA to total
514 $\text{PM}_{2.5}$ far more realistically, compared to observations. As discussed in Sect. 2.3 and Eq. 11,
515 having the model accurately predict the fractional contribution of ASOA to the total PM is very
516 important, as the total $\text{PM}_{2.5}$ is derived from satellite-based estimates (van Donkelaar et al.,
517 2015), and the model fractions are then applied to those total $\text{PM}_{2.5}$ estimates. The ability for the
518 “improved” SIMPLE model to better represent the ASOA composition provides confidence
519 attributing the ASOA contribution to premature mortality.

520

521 **5. Preliminary Evaluation of Worldwide Premature Deaths Due to ASOA with Updated** 522 **SIMPLE Parameterization**

523 The improved SIMPLE parameterization is used along with GEOS-Chem to provide an
524 accurate estimation of ASOA formation in urban areas worldwide and provide an ability to
525 obtain realistic simulations of ASOA based on measurement data. We use this model to quantify

526 the attribution of $PM_{2.5}$ ASOA to premature deaths. Analysis up to this point has been for PM_1 ;
527 however, both the chemical transport model and epidemiological studies utilize $PM_{2.5}$. For
528 ASOA, this will not impact the discussion and results here because the mass of OA (typically
529 80–90%) is dominated by PM_1 (e.g., Bae et al., 2006; Seinfeld and Pandis, 2006), and ASOA is
530 formed mostly through condensation of oxidized species, which favors partitioning onto smaller
531 particles (Seinfeld and Pandis, 2006).

532 The procedure for this analysis is described in Fig. 7 and Sect. 2.3 and S3. Briefly, we
533 combine high-resolution satellite-based $PM_{2.5}$ estimates (for exposure) and a chemical transport
534 model (GEOS-Chem, for fractional composition) to estimate ASOA concentrations and various
535 sensitivity analysis (van Donkelaar et al., 2015). We calculated ~3.3 million premature deaths
536 (using the Integrated Exposure-Response, IER, function) are due to long-term exposure of
537 ambient $PM_{2.5}$ (Fig. S9, Table S16), consistent with recent literature (Cohen et al., 2017).

538 The attribution of ASOA $PM_{2.5}$ premature deaths can be calculated one of two ways: (a)
539 marginal method (Silva et al., 2016) or (b) attributable fraction method (Anenberg et al., 2019).
540 For method (a), it is assumed that a fraction of the ASOA is removed, keeping the rest of the
541 $PM_{2.5}$ components approximately constant, and the change in deaths is calculated from the deaths
542 associated with the total concentration less the deaths calculated using the reduced total $PM_{2.5}$
543 concentrations. For method (b), the health impact is attributed to each $PM_{2.5}$ component by
544 multiplying the total deaths by the fractional contribution of each component to total $PM_{2.5}$. For
545 method (a), the deaths attributed to ASOA are ~340,000 people per year (Fig. 8); whereas, for
546 method (b), the deaths are ~370,000 people per year. Both of these are based on the IER response
547 function (Cohen et al., 2017).

548 Additional recent work (Burnett et al., 2018) has suggested less reduction in the
549 premature deaths versus $PM_{2.5}$ concentration relationship at higher $PM_{2.5}$ concentrations, and
550 lower concentration limits for the threshold below which this relationship is negligible, both of
551 which lead to much higher estimates of $PM_{2.5}$ associated premature deaths. This is generally
552 termed the Global Exposure Mortality Model (GEMM). Using the two attribution methods
553 described above (a and b), the ASOA $PM_{2.5}$ premature deaths are estimated to be ~640,000
554 (method a) and ~900,000 (method b) (Fig. S9 and Fig. S12 and Table S17).

555 Compared to prior studies using chemical transport models to estimate premature deaths
556 associated with ASOA (e.g., Silva et al., 2016; Ridley et al., 2018), which assumed non-volatile
557 POA and “traditional” ASOA precursors, the attribution of premature mortality due to ASOA is
558 over an order of magnitude higher in this study (Fig. 9). This occurs using either the IER and
559 GEMM approach for estimating premature mortality (Fig. 9). For regions with larger populations
560 and more $PM_{2.5}$ pollution, the attribution is between a factor of 40 to 80 higher. This stems from
561 the non-volatile POA and “traditional” ASOA precursors over-estimating POA and
562 under-estimating ASOA compared to observations (Schroder et al., 2018). These offsetting
563 errors will lead to model predicted total OA similar to observations (Ridley et al., 2018; Schroder
564 et al., 2018), yet different conclusions on whether POA versus SOA is more important for
565 reducing $PM_{2.5}$ associated premature mortality. Using a model constrained to day-time
566 atmospheric observations (Fig. 2 and Fig. 4, see Sect. 4) leads to a more accurate than earlier
567 estimation of the contribution of photochemically-produced ASOA to $PM_{2.5}$ associated
568 premature mortality that has not been possible in prior studies. We note that ozone concentrations
569 change little as we change the ASOA simulation (see Sect. S4 and Fig. S14).

570 A limitation in this study is the lack of sufficient measurements in South and Southeast
571 Asia, Eastern Europe, Africa, and South America (Fig. 1), though these areas account for 44% of
572 the predicted reduction in premature mortality for the world (Table S16). However, as
573 highlighted in Table S18, these regions likely still consume both transportation fuels and VCPs,
574 although in lower per capita amounts than more industrialized countries. This consumption is
575 expected to lead to the same types of emissions as for the cities studied here, though more field
576 measurements are needed to validate global inventories of VOCs and resulting oxidation
577 products in the developing world. Transportation emissions of VOCs are expected to be more
578 dominant in the developing world due to higher VOC emission factors associated with inefficient
579 combustion engines, such as two-stroke scooters (Platt et al., 2014) and auto-rickshaws (e.g.,
580 Goel and Guttikunda, 2015).

581 Solid fuels are used for residential heating and cooking, which impact the outdoor air
582 quality as well (Hu et al., 2013, 2016; Lacey et al., 2017; Stewart et al., 2020), and which also
583 lead to SOA (Heringa et al., 2011). As discussed in Sect. 3.1, though the majority of the studies
584 evaluated here occurred in spring to summer time, when solid fuel emissions are decreased, two
585 studies occurred during the winter/early spring time, where solid fuel emissions were important
586 (Hu et al., 2013; Schroder et al., 2018). These studies still follow the same relationship between
587 ASOA and R_{BTEX} as the studies that focused on spring/summer time photochemistry. Thus, the
588 limited datasets available indicate that photochemically produced ASOA from solid fuels follow
589 a similar relationship to that from other ASOA sources.

590 Also, solid fuel sources are included in the inventories used in our modeling. For the
591 HTAP emission inventory used here (Janssens-Maenhout et al., 2015), small-scale combustion,

592 which includes heating and cooking (e.g., solid-fuel use), is included in the residential emission
593 sector. Both CO and BTEX are included in this source, and can account for a large fraction of the
594 total emissions where solid-fuel use may be important (Fig. S15). Thus, as CO and BTEX are
595 used in the updated SIMPLE model, and campaigns that observed solid-fuel emissions fall
596 within the trend for all urban areas, the solid-fuel contribution to photochemically-produced
597 ASOA is accounted for (as accurately as allowed by current datasets) in the estimation of ASOA
598 for the attribution to premature mortality.

599 Note that recent work has observed potential nighttime aqueous chemistry and/or
600 oxidation by nitrate radical from solid fuel emissions to produce ASOA (Kodros et al., 2020).
601 Thus, missing this source of ASOA may lead to an underestimation of total ASOA versus the
602 photochemically-produced ASOA we discuss here, leading to a potential underestimation in the
603 attribution of ASOA to premature mortality. From the studies that investigated “night-time
604 aging” of solid-fuel emissions to form SOA, we predict that the total ASOA may be
605 underestimated by 1 to 3 $\mu\text{g m}^{-3}$ (Kodros et al., 2020). This potential underestimation, though, is
606 less than the current underestimation in ASOA in GEOS-Chem (default versus “Updated”
607 SIMPLE).

608 Recently, emission factors from Abidjan, Côte d’Ivoire, a developing urban area, showed
609 the dominance of emissions from transportation and solid fuel burning, with BTEX being an
610 important fraction of the total emissions, and that all the emissions were efficient in producing
611 ASOA (Dominutti et al., 2019). Further, investigation of emissions in New Delhi region of India
612 demonstrated the importance of both transportation and solid fuel emissions (Stewart et al.,
613 2020; Wang et al., 2020) while model comparisons with observations show an underestimation

614 of OA compared to observations due to a combination of emissions and OA representation (Jena
615 et al., 2020). Despite emission source differences, SOA is still an important component of $PM_{2.5}$
616 (e.g., Singh et al., 2019) and thus will impact air quality and premature mortality in developing
617 regions. Admittedly, though, our estimates will be less accurate for these regions.

618

619 **6. Conclusions**

620 In summary, ASOA is an important, though inadequately constrained component of air
621 pollution in megacities and urban areas around the world. This stems from the complexity
622 associated with the numerous precursor emission sources, chemical reactions, and oxidation
623 products that lead to observed ASOA concentrations. We have shown here that the variability in
624 observed ASOA across urban areas is correlated with R_{BTEX} , a marker for the co-emissions of
625 IVOC from both transportation and VCP emissions. Global simulations indicate ASOA
626 contributes to a substantial fraction of the premature mortality associated with $PM_{2.5}$. Reductions
627 of the ASOA precursors will reduce the premature deaths associated with $PM_{2.5}$, indicating the
628 importance of identifying and reducing exposure to sources of ASOA. These sources include
629 emissions that are both traditional (transportation) as well as non-traditional emissions of
630 emerging importance (VCPs) to ambient $PM_{2.5}$ concentrations in cities around the world. Further
631 investigation of speciated IVOCs and SVOCs for urban areas around the world along with SOA
632 mass concentration and other photochemical products (e.g., O_x , PAN, and HCHO) for other
633 urban areas, especially in South Asia, throughout Africa, and throughout South America, would
634 provide further constraints to improve the SIMPLE model and our understanding of the emission
635 sources and chemistry that leads to the observed SOA and its impact on premature mortality.

636 Acknowledgements

637

638 This study was partially supported by grants from NASA NNX15AT96G, NNX16AQ26G, Sloan
639 Foundation 2016-7173, NSF AGS-1822664, EPA STAR 83587701-0, NERC NE/H003510/1,
640 NERC NE/H003177/1, NERC NE/H003223/1, NOAA NA17OAR4320101, NCAS
641 R8/H12/83/037, Natural Science and Engineering Research Council of Canada (NSERC,
642 RGPIN/05002-2014), and the Fonds de Recherche du Québec —Nature et technologies
643 (FRQNT, 2016-PR-192364). This manuscript has not been formally reviewed by EPA. The
644 views expressed in this document are solely those of the authors and do not necessarily reflect
645 those of the Agency. EPA does not endorse any products or commercial services mentioned in
646 this publication. We thank Katherine Travis for useful discussions. We acknowledge B J. Bandy,
647 J. Lee, G. P. Mills, d. D. Montzka, J. Stutz, A. J. Weinheimer E. J. Williams, E. C. Wood, and D.
648 R. Worsnop for use of their data.

649

650 Data Availability

651 TexAQS measurements are available at
652 <https://esrl.noaa.gov/csl/groups/csl7/measurements/2000TexAQS/LaPorte/DataDownload/> and
653 upon request. NEAQS measurements are available at
654 <https://www.esrl.noaa.gov/csl/groups/csl7/measurements/2002NEAQS/>. MILAGRO
655 measurements are available at <http://doi.org/10.5067/Aircraft/INTEXB/Aerosol-TraceGas>.
656 CalNex measurements are available at
657 <https://esrl.noaa.gov/csl/groups/csl7/measurements/2010calnex/Ground/DataDownload/>.
658 ClearfLo measurements are available at
659 <https://catalogue.ceda.ac.uk/uuid/6a5f9eedd68f43348692b3bace3eba45>. SEAC⁴RS measurements
660 are available at <http://doi.org/10.5067/Aircraft/SEAC4RS/Aerosol-TraceGas-Cloud>. WINTER
661 measurements are available at https://data.eol.ucar.edu/master_lists/generated/winter/.
662 KORUS-AQ measurements are available at
663 <http://doi.org/10.5067/Suborbital/KORUSAQ/DATA01>. Data from Chinese campaigns are
664 available upon request, and rest of data used were located in papers cited. GEOS-Chem data
665 available upon request. Figures will become accessible at
666 cires1.colorado.edu/jimenez/group_pubs.html.

667

668 Competing Interests

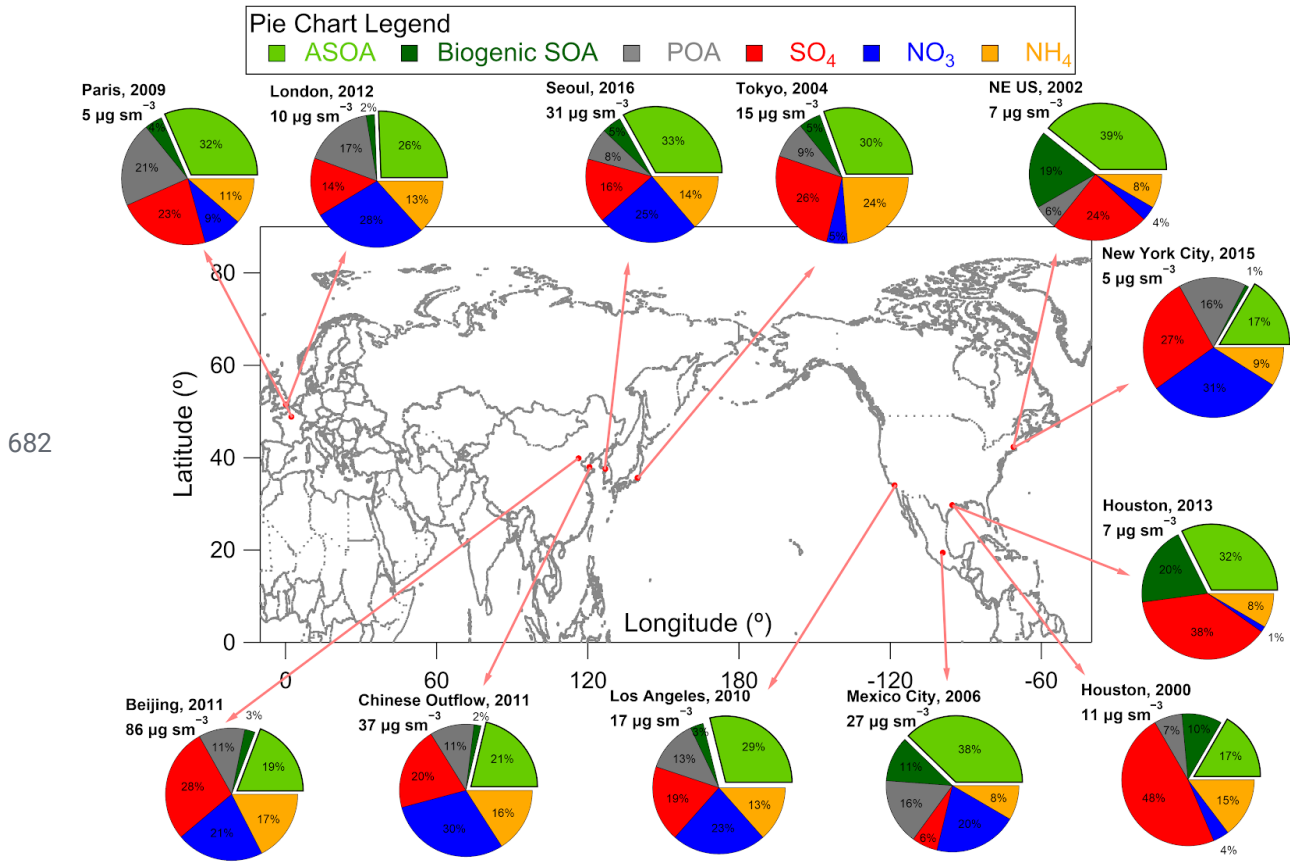
669 The authors declare no competing interests.

670

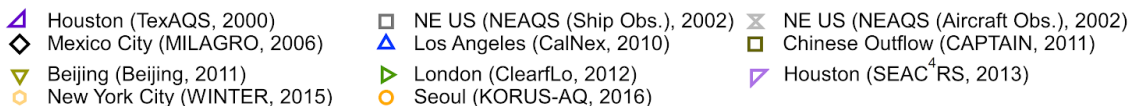
671 Author Contribution

672 B.A.N., D.S.J., B.C.M., J.A.dG., and J.L.J designed the experiment and wrote the paper. B.A.N.,
673 PC.-J., D.A.D., W.H., J.C.S, J.A., D.R.B., M.R.C., H.C., M.M.C., P.F.D, G.S.D., R.D., F.F, A.F.,
674 J.B.G., G.G., J.F.H, T.F.H., P.L.H., J.H., M.H., L.G.H., B.T.J., W.C.K., J.L., I.B.P., J.P., B.R.,

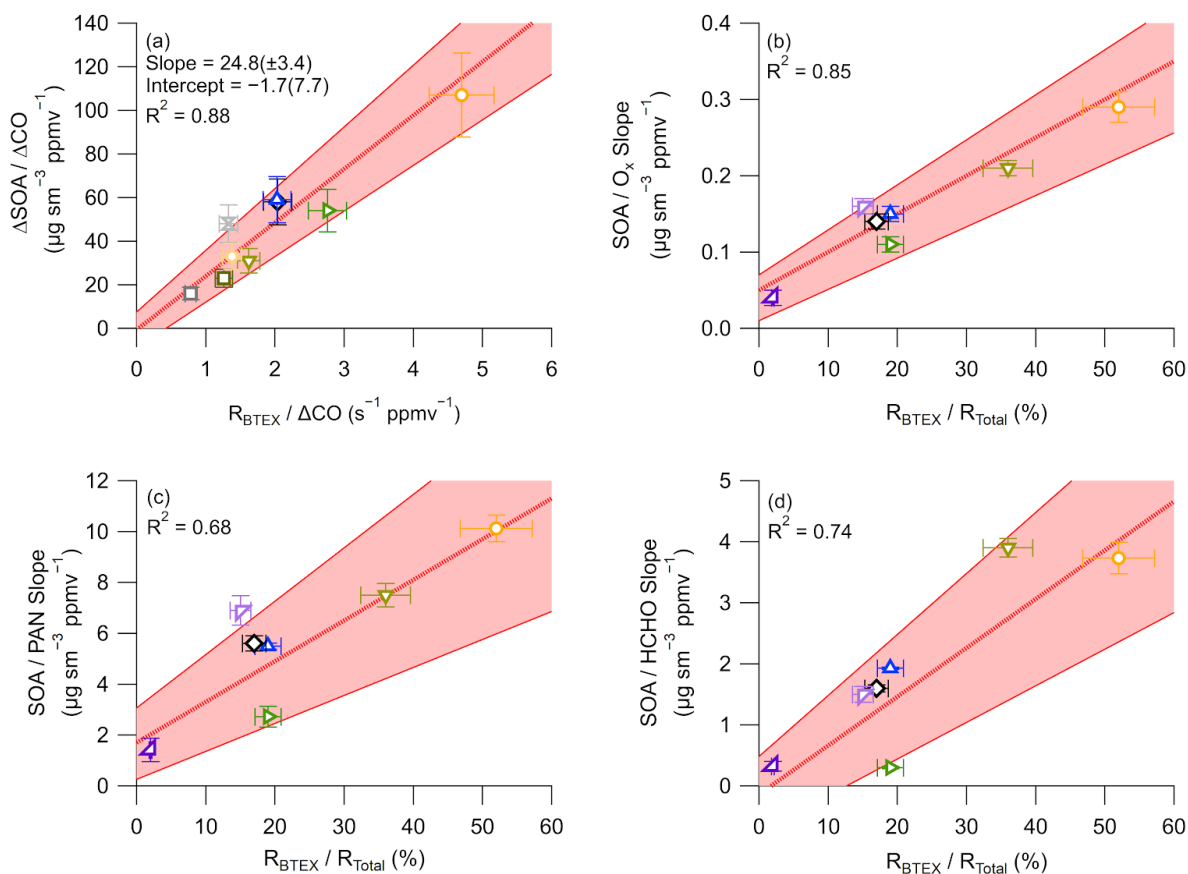
675 C.E.R., D.R., J.M.R., T.B.R, M.S., J.W., C.W., P.W., G.M.W., D.E.Y., B.Y., J.A.dG., and J.L.J.
676 collected and analyzed the data. D.S.J. and A.H. ran the GEOS-Chem model and B.A.N., D.S.J,
677 and J.L.J. analyzed the model output. B.A.N., P.L.H., J.M.S., and J.L.J. ran and analyzed the 0-D
678 model used for ASOA budget analysis of ambient observations. B.C.M., A.L., M.L., and Q.Z.
679 analyzed and provided the emission inventories used for the 0-D box model. D.S.J., D.K.H., and
680 M.O.N. conducted the ASOA attribution to mortality calculation, and B.A.N., D.S.J., D.K.H.,
681 M.O.N., J.A.dG, and J.L.J analyzed the results. All authors reviewed the paper.



683 **Figure 1.** Non-refractory submicron aerosol composition measured in urban and urban outflow
 684 regions from field campaigns used in this study, all in units of $\mu\text{g m}^{-3}$, at standard temperature
 685 (273 K) and pressure (1013 hPa) (sm^{-3}). See Sect. S3 and Table 1 for further information on
 686 measurements, studies, and apportionment of SOA into ASOA and BSOA.

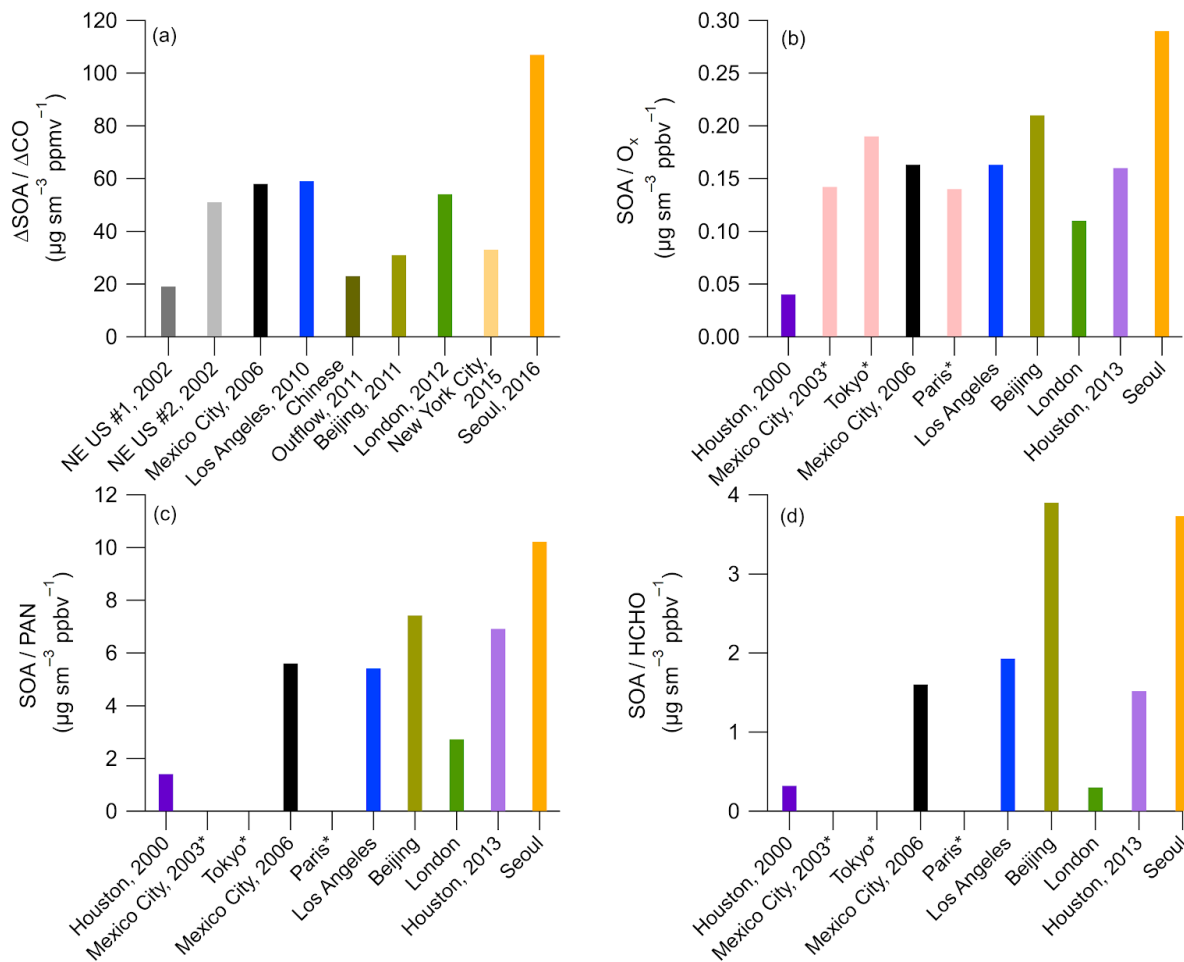


687



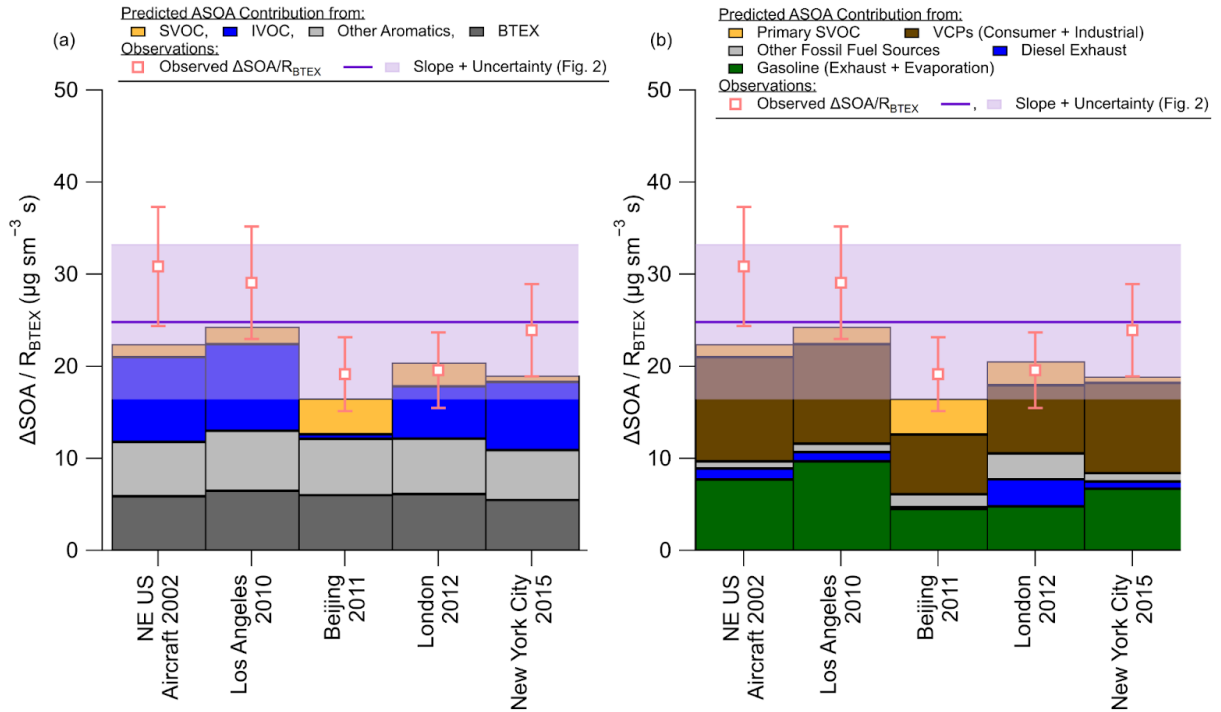
688 **Figure 2.** (a) Scatter plot of background and dilution corrected ASOA concentrations
 689 ($\Delta\text{SOA}/\Delta\text{CO}$ at PA = 0.5 equivalent days) versus BTEX emission reactivity ratio ($R_{\text{BTEX}} =$
 690 $\sum_i [\text{VOC}/\text{CO}]_i$) for multiple major field campaigns on three continents. Comparison of ASOA
 691 versus (b) O_x, (c) PAN, and (d) HCHO slopes versus the ratio of the BTEX/Total emission
 692 reactivity, where total is the OH reactivity for the emissions of BTEX + C2-3 alkenes + C2-6
 693 alkanes (Table S5 through Table S7), for the campaigns studied here. For all figures, red shading
 694 is the $\pm 1\sigma$ uncertainty of the slope, and the bars are $\pm 1\sigma$ uncertainty of the data (see Sect. S5).

695

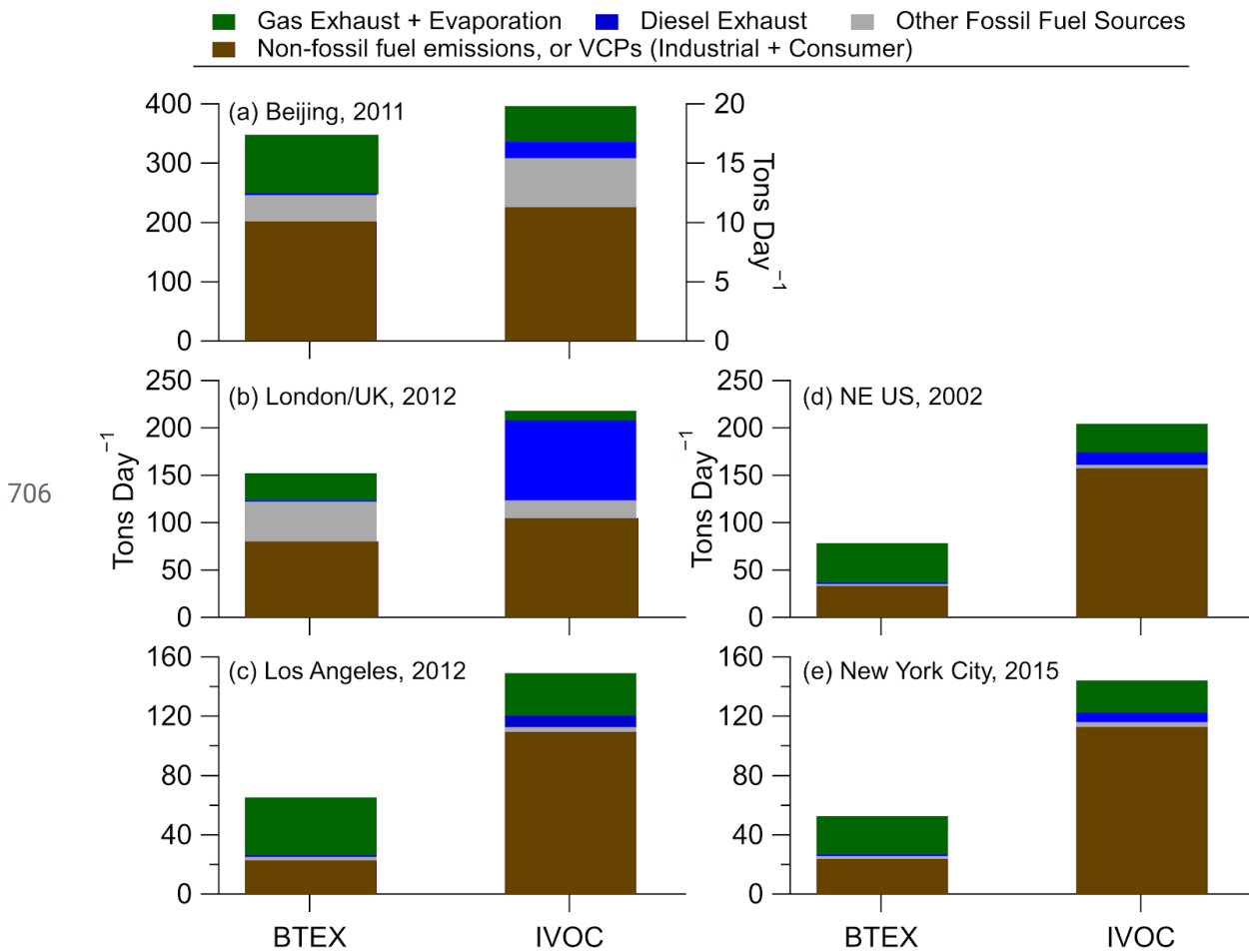


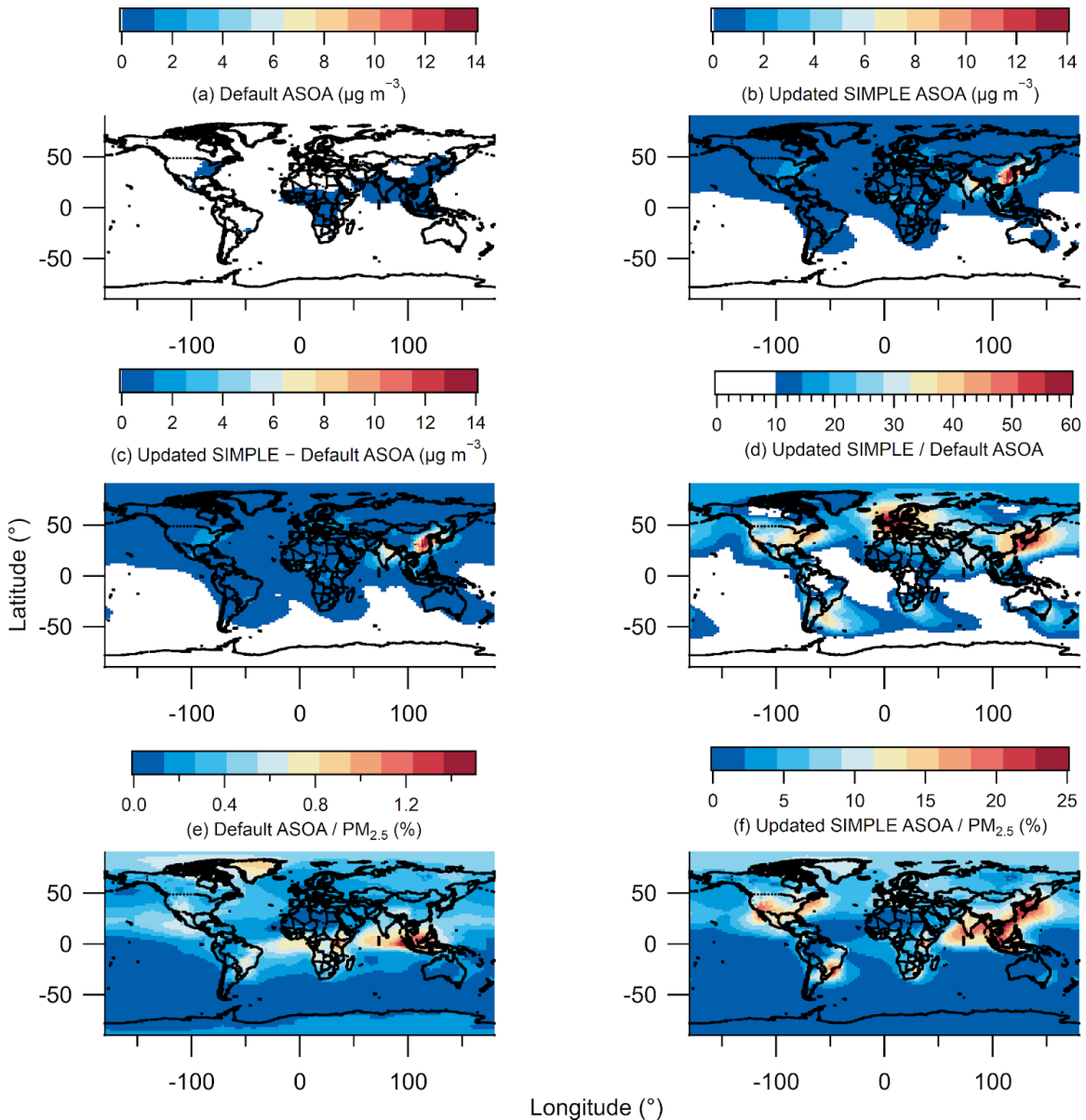
696 **Figure 3.** (a) A comparison of the $\Delta\text{SOA}/\Delta\text{CO}$ for the urban campaigns on three continents.
 697 Comparison of (b) SOA/O_x , (c) SOA/HCHO , and (d) SOA/PAN slopes for the urban areas
 698 (Table S4). For (b) through (d), cities marked with * have no HCHO, PAN, or hydrocarbon data.

699

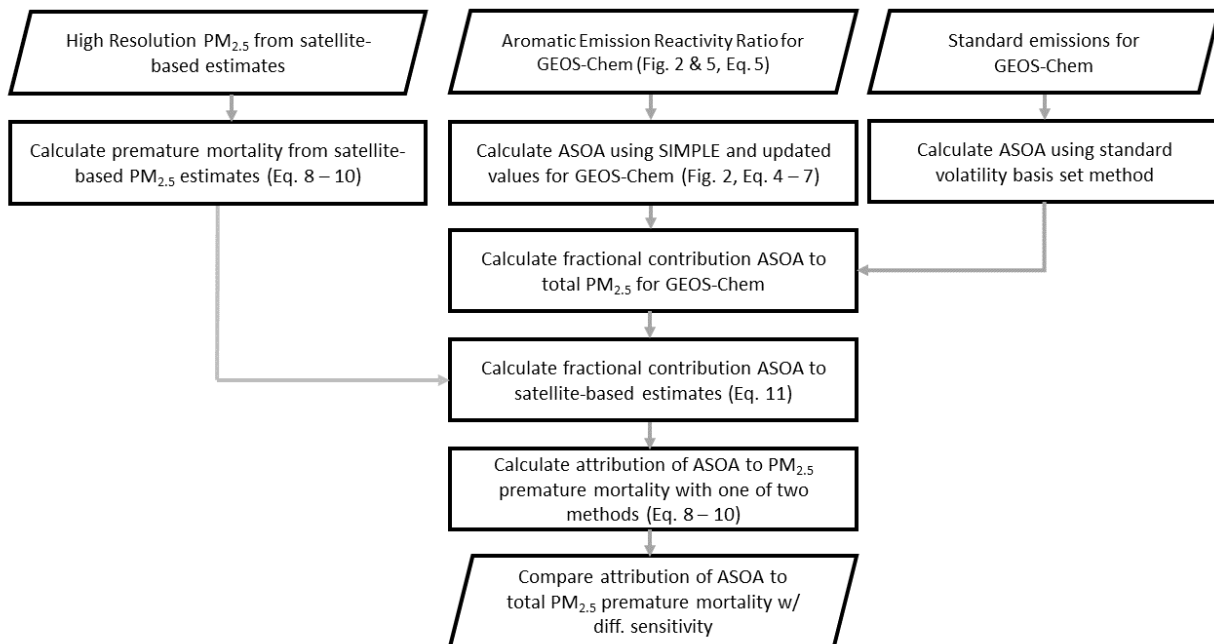


700 **Figure 4.** (a) Budget analysis for the contribution of the observed $\Delta\text{SOA}/R_{\text{BTEX}}$ (Fig. 2) for cities
 701 with known emissions inventories for different volatility classes (see SI and Fig. 5 and Fig. S6).
 702 (b) Same as (a), but for sources of emissions. For (a) and (b), SVOC is the contribution from
 703 both vehicle and other (cooking, etc.) sources. See SI for information about the emissions,
 704 ASOA precursor contribution, error analysis, and discussion about sensitivity of emission
 705 inventory IVOC/BTEX ratios for different cities and years in the US.



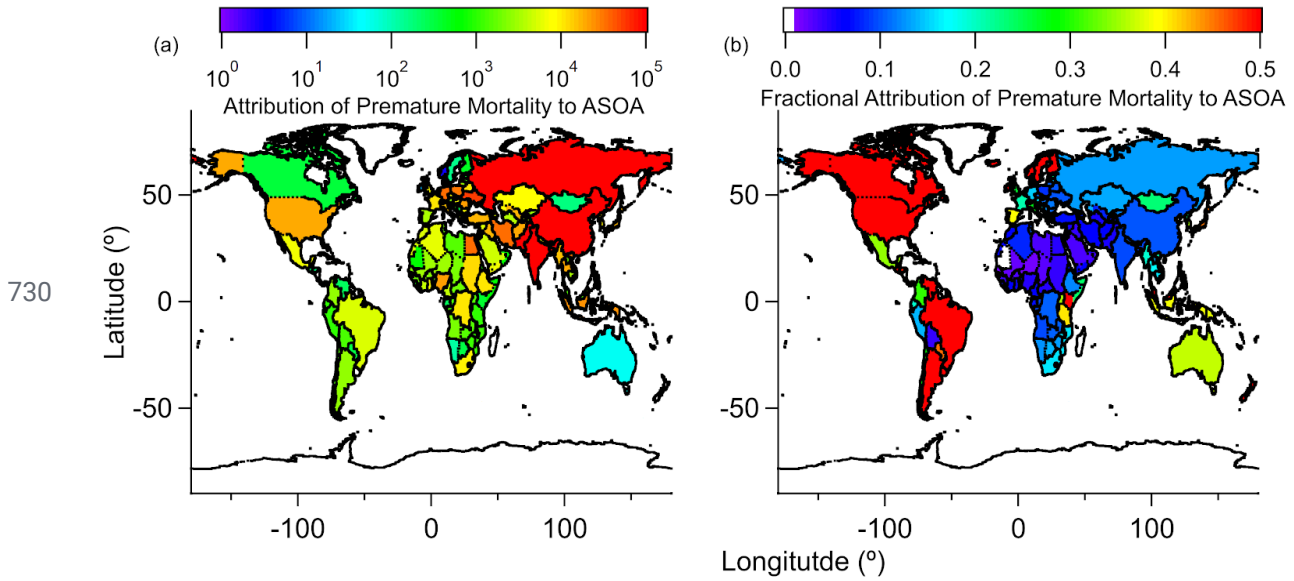


713 **Figure 6.** (a) Annual average modeled ASOA using the default VBS. (b) Annual average
 714 modeled ASOA using the updated SIMPLE model. (c) Difference between annual average
 715 modeled updated SIMPLE and default VBS. Note, for (a) - (b), values less than $0.05 \mu\text{g m}^{-3}$ are
 716 white, and for (c), values less than $0.02 \mu\text{g m}^{-3}$ are white. (d) Ratio between annual average
 717 modeled updated SIMPLE (b) and default VBS (a). (e) Percent contribution of annual average
 718 modeled ASOA using default VBS to total modelled PM_{2.5}. (f) Percent contribution of annual
 719 average modeled ASOA using updated SIMPLE to total modelled PM_{2.5}.

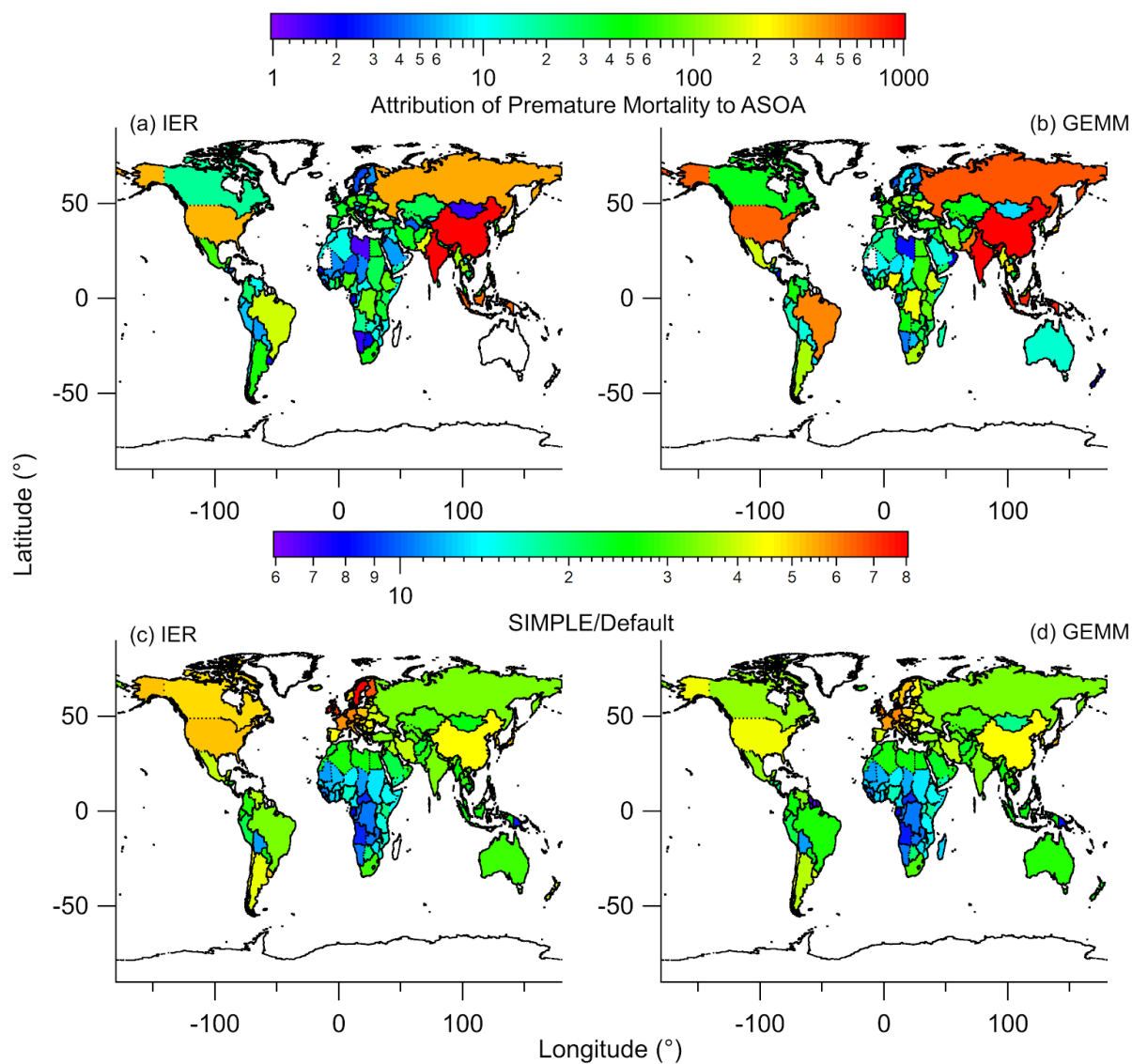


720

721 **Figure 7.** Flowchart describing how observed ASOA production was used to calculate ASOA in
 722 GEOS-Chem, and how the satellite-based PM_{2.5} estimates and GEOS-Chem PM_{2.5} speciation was
 723 used to estimate the premature mortality and attribution of premature mortality by ASOA. See
 724 Sect. 2 and SI for further information about the details in the figure. SIMPLE is described in
 725 Eq. 4 and by Hodzic and Jimenez (2011) and Hayes et al. (2015). The one of two methods
 726 mentioned include either the Integrated Exposure-Response (IER) (Burnett et al., 2014) with
 727 Global Burden of Disease (GBD) dataset (IHME, 2016) or the new Global Exposure Mortality
 728 Model (GEMM) (Burnett et al., 2018) methods. For both IER and GEMM, the marginal method
 729 (Silva et al., 2016) or attributable fraction method (Anenberg et al., 2019) are used.



731 **Figure 8.** Five-year average (a) estimated reduction in $PM_{2.5}$ -associated premature deaths, by
 732 country, upon removing ASOA from total $PM_{2.5}$, and (b) fractional reduction (reduction $PM_{2.5}$
 733 premature deaths / total $PM_{2.5}$ premature deaths) in $PM_{2.5}$ -associated premature deaths, by
 734 country, upon removing ASOA from GEOS-Chem. The IER methods are used here. See Fig. S9
 735 and Fig. S12 for results using GEMM. See Fig. S10 for $10 \times 10 \text{ km}^2$ area results in comparison
 736 with country-level results.



738 **Figure 9.** Attribution of premature mortality to ASOA using (a) IER or (b) GEMM, using the
 739 non-volatile primary OA and traditional SOA precursor method in prior studies (e.g., Ridley et
 740 al., 2018). The increase in attribution of premature mortality to ASOA for the “SIMPLE” model
 741 (Fig. 8) versus the non-volatile primary OA and traditional SOA precursor method (“Default”),
 742 for (c) IER and (d) GEMM.

743 **Table 1.** List of campaigns used here. For values previously reported for those campaigns, they
 744 are noted. For Seasons, W = Winter, Sp = Spring, and Su = Summer.

Location	Field Campaign	Coordinates		Time Period	Season	Previous Publication/Campaign Overview
		Long. (°)	Lat. (°)			
Houston, TX, USA (2000)	TexAQS 2000	-95.4	29.8	15/Aug/2000 - 15/Sept/2000	Su	Jimenez et al. (2009) ^a , Wood et al. (2010) ^b
Northeast USA (2002)	NEAQS 2002	-78.1 - -70.5	32.8 - 43.1	26/July/2002; 29/July/2002 - 10/Aug/2002	Su	Jimenez et al. (2009) ^a , de Gouw and Jimenez (2009) ^c , Kleinman et al. (2007) ^c
Mexico City, Mexico (2003)	MCMA-2003	-99.2	19.5	31/Mar/2003 - 04/May/2003	Sp	Molina et al. (2007), Herndon et al. (2008) ^b
Tokyo, Japan (2004)		139.7	35.7	24/July/2004 - 14/Aug/2004	Su	Kondo et al. (2008) ^a , Miyakawa et al. (2008) ^a , Morino et al. (2014) ^b
Mexico City, Mexico (2006)	MILAGRO	-99.4 - -98.6	19.0 - 19.8	04/Mar/2006 - 29/Mar/2006	Sp	Molina et al. (2010), DeCarlo et al. (2008) ^a , Wood et al. (2010) ^b , DeCarlo et al. (2010) ^c
Paris, France (2009)	MEGAPOLI	48.9	2.4	13/July/2009 - 29/July/2009	Su	Frenay et al. (2014) ^a , Zhang et al. (2015) ^b
Pasadena, CA, USA (2010)	CalNex	-118.1	34.1	15/May/2010 - 16/June/2010	Sp	Ryerson et al. (2013), Hayes et al. (2013) ^{a,b,c}
Changdao Island, China (2011)	CAPTAIN	120.7	38.0	21/Mar/2011 - 24/Apr/2011	Sp	Hu et al. (2013) ^{a,c}
Beijing, China (2011)	CareBeijing 2011	116.4	39.9	03/Aug/2011 - 15/Sept/2011	Su	Hu et al. (2016) ^{a,b,c}
London, UK (2012)	ClearfLo	0.1	51.5	22/July/2012 - 18/Aug/2012	Su	Bohnenstengel et al. (2015)
Houston, TX, USA (2013)	SEAC ⁴ RS	-96.0 - -94.0	29.2 - 30.3	01/Aug/2013 - 23/Sept/2013	Su	Toon et al. (2016)
New York City, NY, USA (2015)	WINTER	-74.0 - -69.0	39.5 - 42.5	07/Feb/2015	W	Schroder et al. (2018) ^{a,c}
Seoul, South Korea (2016)	KORUS-AQ	124.6 - 128.0	36.8 - 37.6	01/May/2016 - 10/June/2016	Sp	Nault et al. (2018) ^{a,b,c,d}

745 ^aReference used for PM₁ composition. ^bReference used for SOA/O_x slope. ^cReference used for
 746 ΔOA/ΔCO value. ^dReference used for SOA/HCHO and SOA/PAN slopes

747 References

- 748 Anenberg, S., Miller, J., Henze, D. and Minjares, R.: A global snapshot of the air
749 pollution-related health impacts of transportation sector emissions in 2010 and 2015, ICCT,
750 Climate & Clean Air Coalition., 2019.
- 751 Atkinson, R. and Arey, J.: Atmospheric Degradation of Volatile Organic Compounds, Chem.
752 Rev., 103, 4605–4638, 2003.
- 753 Atkinson, R., Baulch, D. L., Cox, R. A., Crowley, J. N., Hampson, R. F., Hynes, R. G., Jenkin,
754 M. E., Rossi, M. J., Troe, J. and IUPAC Subcommittee: Evaluated kinetic and photochemical
755 data for atmospheric chemistry: Volume II - gas phase reactions of organic species, Atmos.
756 Chem. Phys., 6(11), 3625–4055, 2006.
- 757 Bae, M.-S., Demerjian, K. L. and Schwab, J. J.: Seasonal estimation of organic mass to organic
758 carbon in PM_{2.5} at rural and urban locations in New York state, Atmos. Environ., 40(39),
759 7467–7479, 2006.
- 760 Baker, K. R., Woody, M. C., Valin, L., Szykman, J., Yates, E. L., Iraci, L. T., Choi, H. D., Soja,
761 A. J., Koplitz, S. N., Zhou, L., Campuzano-Jost, P., Jimenez, J. L. and Hair, J. W.: Photochemical
762 model evaluation of 2013 California wild fire air quality impacts using surface, aircraft, and
763 satellite data, Sci. Total Environ., 637-638, 1137–1149, 2018.
- 764 Bertram, T. H., Perring, A. E., Wooldridge, P. J., Crouse, J. D., Kwan, A. J., Wennberg, P. O.,
765 Scheuer, E., Dibb, J., Avery, M., Sachse, G., Vay, S. A., Crawford, J. H., McNaughton, C. S.,
766 Clarke, A., Pickering, K. E., Fuelberg, H., Huey, G., Blake, D. R., Singh, H. B., Hall, S. R.,
767 Shetter, R. E., Fried, A., Heikes, B. G. and Cohen, R. C.: Direct Measurements of the Convective
768 Recycling of the Upper Troposphere, Science, 315(5813), 816–820, 2007.
- 769 Bohnenstengel, S. I., Belcher, S. E., Aiken, A., Allan, J. D., Allen, G., Bacak, A., Bannan, T. J.,
770 Barlow, J. F., Beddows, D. C. S., Bloss, W. J., Booth, A. M., Chemel, C., Coceal, O., Di Marco,
771 C. F., Dubey, M. K., Faloon, K. H., Fleming, Z. L., Furger, M., Gietl, J. K., Graves, R. R., Green,
772 D. C., Grimmond, C. S. B., Halios, C. H., Hamilton, J. F., Harrison, R. M., Heal, M. R., Heard,
773 D. E., Helfter, C., Herndon, S. C., Holmes, R. E., Hopkins, J. R., Jones, A. M., Kelly, F. J.,
774 Kotthaus, S., Langford, B., Lee, J. D., Leigh, R. J., Lewis, A. C., Lidster, R. T., Lopez-Hilfiker,
775 F. D., McQuaid, J. B., Mohr, C., Monks, P. S., Nemitz, E., Ng, N. L., Percival, C. J., Prévôt, A. S.
776 H., Ricketts, H. M. A., Sokhi, R., Stone, D., Thornton, J. A., Tremper, A. H., Valach, A. C.,
777 Visser, S., Whalley, L. K., Williams, L. R., Xu, L., Young, D. E., Zotter, P., Bohnenstengel, S. I.,
778 Belcher, S. E., Aiken, A., Allan, J. D., Allen, G., Bacak, A., Bannan, T. J., Barlow, J. F.,
779 Beddows, D. C. S., Bloss, W. J., Booth, A. M., Chemel, C., Coceal, O., Marco, C. F. D., Dubey,
780 M. K., Faloon, K. H., Fleming, Z. L., Furger, M., Gietl, J. K., Graves, R. R., Green, D. C.,
781 Grimmond, C. S. B., Halios, C. H., Hamilton, J. F., Harrison, R. M., Heal, M. R., Heard, D. E.,
782 Helfter, C., Herndon, S. C., Holmes, R. E., Hopkins, J. R., Jones, A. M., Kelly, F. J., Kotthaus,
783 S., Langford, B., Lee, J. D., Leigh, R. J., Lewis, A. C., Lidster, R. T., Lopez-Hilfiker, F. D., et al.:
784 Meteorology, Air Quality, and Health in London: The ClearfLo Project, Bull. Am. Meteorol.

785 Soc., 96(5), 779–804, 2015.

786 Burnett, R., Chen, H., Szyszkowicz, M., Fann, N., Hubbell, B., Pope, C. A., Apte, J. S., Brauer,
787 M., Cohen, A., Weichenthal, S., Coggins, J., Di, Q., Brunekreef, B., Frostad, J., Lim, S. S., Kan,
788 H., Walker, K. D., Thurston, G. D., Hayes, R. B., Lim, C. C., Turner, M. C., Jerrett, M., Krewski,
789 D., Gapstur, S. M., Diver, W. R., Ostro, B., Goldberg, D., Crouse, D. L., Martin, R. V., Peters, P.,
790 Pinault, L., Tjepkema, M., van Donkelaar, A., Villeneuve, P. J., Miller, A. B., Yin, P., Zhou, M.,
791 Wang, L., Janssen, N. A. H., Marra, M., Atkinson, R. W., Tsang, H., Quoc Thach, T., Cannon, J.
792 B., Allen, R. T., Hart, J. E., Laden, F., Cesaroni, G., Forastiere, F., Weinmayr, G., Jaensch, A.,
793 Nagel, G., Concin, H. and Spadaro, J. V.: Global estimates of mortality associated with long-term
794 exposure to outdoor fine particulate matter, *Proc. Natl. Acad. Sci. U. S. A.*, 115(38), 9592–9597,
795 2018.

796 Burnett, R. T., Pope, C. A., Ezzati, M., Olives, C., Lim, S. S., Mehta, S., Shin, H. H., Singh, G.,
797 Hubbell, B., Brauer, M., Anderson, H. R., Smith, K. R., Balmes, J. R., Bruce, N. G., Kan, H.,
798 Laden, F., Prüss-Ustün, A., Turner, M. C., Gapstur, S. M., Diver, W. R. and Cohen, A.: An
799 integrated risk function for estimating the global burden of disease attributable to ambient fine
800 particulate matter exposure, *Environ. Health Perspect.*, 122(4), 397–403, 2014.

801 Cappa, C. D., Jathar, S. H., Kleeman, M. J., Docherty, K. S., Jimenez, J. L., Seinfeld, J. H. and
802 Wexler, A. S.: Simulating secondary organic aerosol in a regional air quality model using the
803 statistical oxidation model - Part 2: Assessing the influence of vapor wall losses, *Atmos. Chem.*
804 *Phys.*, 16(5), 3041–3059, 2016.

805 Chafe, Z., Brauer, M., Heroux, M.-E., Klimont, Z., Lanki, T., Salonen, R. O. and Smith, K. R.:
806 Residential heating with wood and coal: Health impacts and policy options in Europe and North
807 America, WHO/UNECE LRTAP., 2015.

808 CIESIN: Gridded Population of the World (GPW), v4, SEDAC [online] Available from:
809 <https://sedac.ciesin.columbia.edu/data/collection/gpw-v4> (Accessed 12 May 2020), 2017.

810 Coggon, M. M., McDonald, B. C., Vlasenko, A., Veres, P. R., Bernard, F., Koss, A. R., Yuan, B.,
811 Gilman, J. B., Peischl, J., Aikin, K. C., DuRant, J., Warneke, C., Li, S.-M. and de Gouw, J. A.:
812 Diurnal Variability and Emission Pattern of Decamethylcyclopentasiloxane (D₁₀) from the
813 Application of Personal Care Products in Two North American Cities, *Environ. Sci. Technol.*,
814 52(10), 5610–5618, 2018.

815 Cohen, A. J., Brauer, M., Burnett, R., Anderson, H. R., Frostad, J., Estep, K., Balakrishnan, K.,
816 Brunekreef, B., Dandona, L., Dandona, R., Feigin, V., Freedman, G., Hubbell, B., Jobling, A.,
817 Kan, H., Knibbs, L., Liu, Y., Martin, R., Morawska, L., Pope, C. A., Shin, H., Straif, K.,
818 Shaddick, G., Thomas, M., van Dingenen, R., van Donkelaar, A., Vos, T., Murray, C. J. L. and
819 Forouzanfar, M. H.: Estimates and 25-year trends of the global burden of disease attributable to
820 ambient air pollution: an analysis of data from the Global Burden of Diseases Study 2015,
821 *Lancet*, 389(10082), 1907–1918, 2017.

822 DeCarlo, P. F., Dunlea, E. J., Kimmel, J. R., Aiken, A. C., Sueper, D., Crounse, J., Wennberg, P.

823 O., Emmons, L., Shinozuka, Y., Clarke, A., Zhou, J., Tomlinson, J., Collins, D. R., Knapp, D.,
824 Weinheimer, A. J., Montzka, D. D., Campos, T. and Jimenez, J. L.: Fast airborne aerosol size and
825 chemistry measurements above Mexico City and Central Mexico during the MILAGRO
826 campaign, *Atmos. Chem. Phys.*, 8(14), 4027–4048, 2008.

827 DeCarlo, P. F., Ulbrich, I. M., Crouse, J., de Foy, B., Dunlea, E. J., Aiken, A. C., Knapp, D.,
828 Weinheimer, A. J., Campos, T., Wennberg, P. O. and Jimenez, J. L.: Investigation of the sources
829 and processing of organic aerosol over the Central Mexican Plateau from aircraft measurements
830 during MILAGRO, *Atmos. Chem. Phys.*, 10(12), 5257–5280, 2010.

831 Deming, B., Pagonis, D., Liu, X., Talukdar, R. K., Roberts, J. M., Veres, P. R., Krechmer, J. E.,
832 de Gouw, J. A., Jimenez, J. L. and Ziemann, P. J.: Measurements of Delays of Gas-Phase
833 Compounds in a Wide Variety of Tubing Materials due to Gas-Wall Partitioning, *Atmos. Meas.*
834 *Tech.*, In Prep., 2018.

835 Dominutti, P., Keita, S., Bahino, J., Colomb, A., Lioussé, C., Yoboué, V., Galy-Lacaux, C.,
836 Morris, E., Bouvier, L., Sauvage, S. and Borbon, A.: Anthropogenic VOCs in Abidjan, southern
837 West Africa: from source quantification to atmospheric impacts, *Atmos. Chem. Phys.*, 19(18),
838 11721–11741, 2019.

839 van Donkelaar, A., Martin, R. V., Brauer, M. and Boys, B. L.: Use of Satellite Observations for
840 Long-Term Exposure Assessment of Global Concentrations of Fine Particulate Matter, *Environ.*
841 *Health Perspect.*, 123(2), 135–143, 2015.

842 van Donkelaar, A., Martin, R. V., Brauer, M., Hsu, N. C., Kahn, R. A., Levy, R. C., Lyapustin,
843 A., Sayer, A. M. and Winker, D. M.: Global Estimates of Fine Particulate Matter using a
844 Combined Geophysical-Statistical Method with Information from Satellites, Models, and
845 Monitors, *Environ. Sci. Technol.*, 50(7), 3762–3772, 2016.

846 Dzepina, K., Volkamer, R. M., Madronich, S., Tulet, P., Ulbrich, I. M., Zhang, Q., Cappa, C. D.,
847 Ziemann, P. J. and Jimenez, J. L.: Evaluation of recently-proposed secondary organic aerosol
848 models for a case study in Mexico City, *Atmos. Chem. Phys.*, 9(15), 5681–5709, 2009.

849 EMEP/EEA: EMEP/EEA Air Pollutant Emission Inventory Guidebook 2016, EEA,
850 Luxembourg., 2016.

851 Ensberg, J. J., Hayes, P. L., Jimenez, J. L., Gilman, J. B., Kuster, W. C., de Gouw, J. A.,
852 Holloway, J. S., Gordon, T. D., Jathar, S., Robinson, A. L. and Seinfeld, J. H.: Emission factor
853 ratios, SOA mass yields, and the impact of vehicular emissions on SOA formation, *Atmos.*
854 *Chem. Phys.*, 14(5), 2383–2397, 2014.

855 Freney, E. J., Sellegri, K., Canonaco, F., Colomb, A., Borbon, A., Michoud, V., Crumeyrolle, S.,
856 Amarouche, N., Bourianne, T., Gomes, L., Prevot, A. S. H., Beekmann, M. and
857 Schwarzenböeck, A.: Characterizing the impact of urban emissions on regional aerosol particles:
858 Airborne measurements during the MEGAPOLI experiment, *Atmos. Chem. Phys.*, 14(3),
859 1397–1412, 2014.

860 Gentner, D. R., Isaacman, G., Worton, D. R., Chan, A. W. H., Dallmann, T. R., Davis, L., Liu, S.,
861 Day, D. A., Russell, L. M., Wilson, K. R., Weber, R., Guha, A., Harley, R. A. and Goldstein, A.
862 H.: Elucidating secondary organic aerosol from diesel and gasoline vehicles through detailed
863 characterization of organic carbon emissions, *Proc. Natl. Acad. Sci. U. S. A.*, 109(45),
864 18318–18323, 2012.

865 Goel, R. and Guttikunda, S. K.: Evolution of on-road vehicle exhaust emissions in Delhi, *Atmos.*
866 *Environ.*, 105, 78–90, 2015.

867 de Gouw, J. A. and Jimenez, J. L.: Organic Aerosols in the Earth's Atmosphere, *Environ. Sci.*
868 *Technol.*, 43(20), 7614–7618, 2009.

869 de Gouw, J. A., Middlebrook, A. M., Warneke, C., Goldan, P. D., Kuster, W. C., Roberts, J. M.,
870 Fehsenfeld, F. C., Worsnop, D. R., Canagaratna, M. R., Pszenny, A. A. P., Keene, W. C.,
871 Marchewka, M., Bertman, S. B. and Bates, T. S.: Budget of organic carbon in a polluted
872 atmosphere: Results from the New England Air Quality Study in 2002, *J. Geophys. Res. D:*
873 *Atmos.*, 110(16), 1–22, 2005.

874 de Gouw, J. A., Gilman, J. B., Kim, S.-W., Lerner, B. M., Isaacman-VanWertz, G., McDonald, B.
875 C., Warneke, C., Kuster, W. C., Lefer, B. L., Griffith, S. M., Dusanter, S., Stevens, P. S. and
876 Stutz, J.: Chemistry of Volatile Organic Compounds in the Los Angeles basin: Nighttime
877 Removal of Alkenes and Determination of Emission Ratios, *J. Geophys. Res.: Atmos.*, 122(21),
878 11,843–11,861, 2017.

879 de Gouw, J. A., Gilman, J. B., Kim, S.-W., Alvarez, S. L., Dusanter, S., Graus, M., Griffith, S.
880 M., Isaacman-VanWertz, G., Kuster, W. C., Lefer, B. L., Lerner, B. M., McDonald, B. C.,
881 Rappenglück, B., Roberts, J. M., Stevens, P. S., Stutz, J., Thalman, R., Veres, P. R., Volkamer, R.,
882 Warneke, C., Washenfelder, R. A. and Young, C. J.: Chemistry of volatile organic compounds in
883 the Los Angeles basin: Formation of oxygenated compounds and determination of emission
884 ratios, *J. Geophys. Res.*, 123(4), 2298–2319, 2018.

885 Grieshop, A. P., Logue, J. M., Donahue, N. M. and Robinson, A. L.: Laboratory investigation of
886 photochemical oxidation of organic aerosol from wood fires 1: measurement and simulation of
887 organic aerosol evolution, *Atmos. Chem. Phys.*, 9(4), 1263–1277, 2009.

888 Hallquist, M., Wenger, J. C., Baltensperger, U., Rudich, Y., Simpson, D., Claeys, M., Dommen,
889 J., Donahue, N. M., George, C., Goldstein, A. H., Hamilton, J. F., Herrmann, H., Hoffmann, T.,
890 Iinuma, Y., Jang, M., Jenkin, M. E., Jimenez, J. L., Kiendler-Scharr, A., Maenhaut, W.,
891 McFiggans, G., Mentel, T. F., Monod, A., Prévôt, A. S. H., Seinfeld, J. H., Surratt, J. D.,
892 Szmigielski, R. and Wildt, J.: The formation, properties and impact of secondary organic aerosol:
893 current and emerging issues, *Atmos. Chem. Phys.*, 9(14), 5155–5236, 2009.

894 Hayes, P. L., Ortega, A. M., Cubison, M. J., Froyd, K. D., Zhao, Y., Cliff, S. S., Hu, W. W.,
895 Toohey, D. W., Flynn, J. H., Lefer, B. L., Grossberg, N., Alvarez, S., Rappenglück, B., Taylor, J.
896 W., Allan, J. D., Holloway, J. S., Gilman, J. B., Kuster, W. C., de Gouw, J. A., Massoli, P.,
897 Zhang, X., Liu, J., Weber, R. J., Corrigan, A. L., Russell, L. M., Isaacman, G., Worton, D. R.,

898 Kreisberg, N. M., Goldstein, A. H., Thalman, R., Waxman, E. M., Volkamer, R., Lin, Y. H.,
899 Surratt, J. D., Kleindienst, T. E., Offenberg, J. H., Dusanter, S., Griffith, S., Stevens, P. S.,
900 Brioude, J., Angevine, W. M. and Jimenez, J. L.: Organic aerosol composition and sources in
901 Pasadena, California, during the 2010 CalNex campaign, *J. Geophys. Res. D: Atmos.*, 118(16),
902 9233–9257, 2013.

903 Hayes, P. L., Carlton, A. G., Baker, K. R., Ahmadov, R., Washenfelder, R. A., Alvarez, S.,
904 Rappenglück, B., Gilman, J. B., Kuster, W. C., de Gouw, J. A., Zotter, P., Prévôt, A. S. H.,
905 Szidat, S., Kleindienst, T. E., Ma, P. K. and Jimenez, J. L.: Modeling the formation and aging of
906 secondary organic aerosols in Los Angeles during CalNex 2010, *Atmos. Chem. Phys.*, 15(10),
907 5773–5801, 2015.

908 Heringa, M. F., DeCarlo, P. F., Chirico, R., Tritscher, T., Dommen, J., Weingartner, E., Richter,
909 R., Wehrle, G., Prévôt, A. S. H. and Baltensperger, U.: Investigations of primary and secondary
910 particulate matter of different wood combustion appliances with a high-resolution time-of-flight
911 aerosol mass spectrometer, *Atmos. Chem. Phys.*, 11(12), 5945–5957, 2011.

912 Herndon, S. C., Onasch, T. B., Wood, E. C., Kroll, J. H., Canagaratna, M. R., Jayne, J. T.,
913 Zavala, M. A., Knighton, W. B., Mazzoleni, C., Dubey, M. K., Ulbrich, I. M., Jimenez, J. L.,
914 Seila, R., de Gouw, J. A., de Foy, B., Fast, J., Molina, L. T., Kolb, C. E. and Worsnop, D. R.:
915 Correlation of secondary organic aerosol with odd oxygen in Mexico City, *Geophys. Res. Lett.*,
916 35(15), L15804, 2008.

917 Hodzic, A. and Jimenez, J. L.: Modeling anthropogenically controlled secondary organic
918 aerosols in a megacity: A simplified framework for global and climate models, *Geosci. Model*
919 *Dev.*, 4(4), 901–917, 2011.

920 Hodzic, A., Jimenez, J. L., Madronich, S., Aiken, A. C., Bessagnet, B., Curci, G., Fast, J.,
921 Lamarque, J.-F., Onasch, T. B., Roux, G., Schauer, J. J., Stone, E. A. and Ulbrich, I. M.:
922 Modeling organic aerosols during MILAGRO: importance of biogenic secondary organic
923 aerosols, *Atmos. Chem. Phys.*, 9(18), 6949–6981, 2009.

924 Hodzic, A., Jimenez, J. L., Prévôt, A. S. H., Szidat, S., Fast, J. D. and Madronich, S.: Can 3-D
925 models explain the observed fractions of fossil and non-fossil carbon in and near Mexico City?,
926 *Atmos. Chem. Phys.*, 10(22), 10997–11016, 2010a.

927 Hodzic, A., Jimenez, J. L., Madronich, S., Canagaratna, M. R., DeCarlo, P. F., Kleinman, L. and
928 Fast, J.: Modeling organic aerosols in a megacity: potential contribution of semi-volatile and
929 intermediate volatility primary organic compounds to secondary organic aerosol formation,
930 *Atmos. Chem. Phys.*, 10(12), 5491–5514, 2010b.

931 Hodzic, A., Campuzano-Jost, P., Bian, H., Chin, M., Colarco, P. R., Day, D. A., Froyd, K. D.,
932 Heinold, B., Jo, D. S., Katich, J. M., Kodros, J. K., Nault, B. A., Pierce, J. R., Ray, E., Schacht,
933 J., Schill, G. P., Schroder, J. C., Schwarz, J. P., Sueper, D. T., Tegen, I., Tilmes, S., Tsigaridis, K.,
934 Yu, P. and Jimenez, J. L.: Characterization of Organic Aerosol across the Global Remote
935 Troposphere: A comparison of ATOM measurements and global chemistry models, *Atmos.*

936 Chem. Phys., 20(8), 4607–4635, 2020.

937 Hu, W., Hu, M., Hu, W., Jimenez, J. L., Yuan, B., Chen, W., Wang, M., Wu, Y., Chen, C., Wang,
938 Z., Peng, J., Zeng, L. and Shao, M.: Chemical composition, sources, and aging process of
939 submicron aerosols in Beijing: Contrast between summer and winter, J. Geophys. Res. D:
940 Atmos., 121(4), 1955–1977, 2016.

941 Hu, W., Downward, G., Wong, J. Y. Y., Reiss, B., Rothman, N., Portengen, L., Li, J., Jones, R.
942 R., Huang, Y., Yang, K., Chen, Y., Xu, J., He, J., Bassig, B., Seow, W. J., Hosgood, H. D., Zhang,
943 L., Wu, G., Wei, F., Vermeulen, R. and Lan, Q.: Characterization of outdoor air pollution from
944 solid fuel combustion in Xuanwei and Fuyuan, a rural region of China, Sci. Rep., 10(1), 11335,
945 2020.

946 Hu, W. W., Hu, M., Yuan, B., Jimenez, J. L., Tang, Q., Peng, J. F., Hu, W., Shao, M., Wang, M.,
947 Zeng, L. M., Wu, Y. S., Gong, Z. H., Huang, X. F. and He, L. Y.: Insights on organic aerosol
948 aging and the influence of coal combustion at a regional receptor site of central eastern China,
949 Atmos. Chem. Phys., 13(19), 10095–10112, 2013.

950 IHME: Global Burden of Disease Study 2015 (GBD 2015) Data Resources, GHDx [online]
951 Available from: <http://ghdx.healthdata.org/gbd-2015> (Accessed 2019), 2016.

952 Janssen, R. H. H., Tsimpidi, A. P., Karydis, V. A., Pozzer, A., Lelieveld, J., Crippa, M., Prévôt,
953 A. S. H., Ait-Helal, W., Borbon, A., Sauvage, S. and Locoge, N.: Influence of local production
954 and vertical transport on the organic aerosol budget over Paris, J. Geophys. Res. D: Atmos.,
955 122(15), 8276–8296, 2017.

956 Janssens-Maenhout, G., Crippa, M., Guizzardi, D., Dentener, F., Muntean, M., Pouliot, G.,
957 Keating, T., Zhang, Q., Kurokawa, J., Wankmüller, R., Denier van der Gon, H., Kuenen, J. J. P.,
958 Klimont, Z., Frost, G., Darras, S., Koffi, B. and Li, M.: HTAP_v2.2: a mosaic of regional and
959 global emission grid maps for 2008 and 2010 to study hemispheric transport of air pollution,
960 Atmos. Chem. Phys., 15(19), 11411–11432, 2015.

961 Jathar, S. H., Woody, M., Pye, H. O. T., Baker, K. R. and Robinson, A. L.: Chemical transport
962 model simulations of organic aerosol in southern California: model evaluation and gasoline and
963 diesel source contributions, Atmos. Chem. Phys., 17(6), 4305–4318, 2017.

964 Jena, C., Ghude, S. D., Kulkarni, R., Debnath, S., Kumar, R., Soni, V. K., Acharja, P., Kulkarni,
965 S. H., Khare, M., Kaginalkar, A. J., Chate, D. M., Ali, K., Nanjundiah, R. S. and Rajeevan, M.
966 N.: Evaluating the sensitivity of fine particulate matter (PM_{2.5}) simulations to chemical
967 mechanism in Delhi, Atmos. Chem. Phys. Discuss., doi:10.5194/acp-2020-673, 2020.

968 Jimenez, J. L., Canagaratna, M. R., Donahue, N. M., Prevot, A. S. H., Zhang, Q., Kroll, J. H.,
969 DeCarlo, P. F., Allan, J. D., Coe, H., Ng, N. L., Aiken, A. C., Docherty, K. S., Ulbrich, I. M.,
970 Grieshop, A. P., Robinson, A. L., Duplissy, J., Smith, J. D., Wilson, K. R., Lanz, V. A., Hueglin,
971 C., Sun, Y. L., Tian, J., Laaksonen, A., Raatikainen, T., Rautiainen, J., Vaattovaara, P., Ehn, M.,
972 Kulmala, M., Tomlinson, J. M., Collins, D. R., Cubison, M. J., Dunlea, E. J., Huffman, J. A.,

973 Onasch, T. B., Alfarra, M. R., Williams, P. I., Bower, K., Kondo, Y., Schneider, J., Drewnick, F.,
974 Borrmann, S., Weimer, S., Demerjian, K., Salcedo, D., Cottrell, L., Griffin, R., Takami, A.,
975 Miyoshi, T., Hatakeyama, S., Shimono, A., Sun, J. Y., Zhang, Y. M., Dzepina, K., Kimmel, J. R.,
976 Sueper, D., Jayne, J. T., Herndon, S. C., Trimborn, A. M., Williams, L. R., Wood, E. C.,
977 Middlebrook, A. M., Kolb, C. E., Baltensperger, U. and Worsnop, D. R.: Evolution of organic
978 aerosols in the atmosphere, *Science*, 326(5959), 1525–1529, 2009.

979 Khare, P. and Gentner, D. R.: Considering the future of anthropogenic gas-phase organic
980 compound emissions and the increasing influence of non-combustion sources on urban air
981 quality, *Atmos. Chem. Phys.*, 18(8), 5391–5413, 2018.

982 Khare, P., Machesky, J., Soto, R., He, M., Presto, A. A. and Gentner, D. R.: Asphalt-related
983 emissions are a major missing nontraditional source of secondary organic aerosol precursors, *Sci*
984 *Adv*, 6(36), doi:10.1126/sciadv.abb9785, 2020.

985 Kleinman, L. I., Daum, P. H., Lee, Y.-N., Senum, G. I., Springston, S. R., Wang, J., Berkowitz,
986 C., Hubbe, J., Zaveri, R. A., Brechtel, F. J., Jayne, J., Onasch, T. B. and Worsnop, D.: Aircraft
987 observations of aerosol composition and ageing in New England and Mid-Atlantic States during
988 the summer 2002 New England Air Quality Study field campaign, *J. Geophys. Res. D: Atmos.*,
989 112(D9), D09310, 2007.

990 Kodros, J. K., Carter, E., Brauer, M., Volckens, J., Bilsback, K. R., L'Orange, C., Johnson, M.
991 and Pierce, J. R.: Quantifying the Contribution to Uncertainty in Mortality Attributed to
992 Household, Ambient, and Joint Exposure to PM_{2.5} From Residential Solid Fuel Use, *Geohealth*,
993 2(1), 25–39, 2018.

994 Kodros, J. K., Papanastasiou, D. K., Paglione, M., Masiol, M., Squizzato, S., Florou, K.,
995 Skyllakou, K., Kaltsonoudis, C., Nenes, A. and Pandis, S. N.: Rapid dark aging of biomass
996 burning as an overlooked source of oxidized organic aerosol, *Proc. Natl. Acad. Sci. U. S. A.*,
997 117(52), 33028–33033, 2020.

998 Kondo, Y., Morino, Y., Fukuda, M., Kanaya, Y., Miyazaki, Y., Takegawa, N., Tanimoto, H.,
999 McKenzie, R., Johnston, P., Blake, D. R., Murayama, T. and Koike, M.: Formation and transport
1000 of oxidized reactive nitrogen, ozone, and secondary organic aerosol in Tokyo, *J. Geophys. Res.*
1001 *D: Atmos.*, 113(D21), D21310, 2008.

1002 Krechmer, J. E., Pagonis, D., Ziemann, P. J. and Jimenez, J. L.: Quantification of Gas-Wall
1003 Partitioning in Teflon Environmental Chambers Using Rapid Bursts of Low-Volatility Oxidized
1004 Species Generated in Situ, *Environ. Sci. Technol.*, 50(11), 5757–5765, 2016.

1005 Krewski, D., Jerrett, M., Burnett, R. T., Ma, R., Hughes, E., Shi, Y., Turner, M. C., Arden, C.,
1006 Thurston, G., Calle, E. E., Thun, M. J., Beckerman, B., Deluca, P., Finkelstein, N., Ito, K.,
1007 Moore, D. K., Newbold, K. B., Ramsay, T., Ross, Z., Shin, H. and Tempalski, B.: Extended
1008 Follow-Up and Spatial Analysis of the American Cancer Society Study Linking Particulate Air
1009 Pollution and Mortality Number 140 May 2009 PRESS VERSION., 2009.

1010 Lacey, F. G., Henze, D. K., Lee, C. J., van Donkelaar, A. and Martin, R. V.: Transient climate
1011 and ambient health impacts due to national solid fuel cookstove emissions, *Proc. Natl. Acad. Sci.*
1012 *U. S. A.*, 114(6), 1269–1274, 2017.

1013 Lam, N. L., Upadhyay, B., Maharjan, S., Jagoe, K., Weyant, C. L., Thompson, R., Uprety, S.,
1014 Johnson, M. A. and Bond, T. C.: Seasonal fuel consumption, stoves, and end-uses in rural
1015 households of the far-western development region of Nepal, *Environ. Res. Lett.*, 12(12), 125011,
1016 2017.

1017 Landrigan, P. J., Fuller, R., Acosta, N. J. R., Adeyi, O., Arnold, R., Basu, N., Baldé, A. B.,
1018 Bertollini, R., Bose-O'Reilly, S., Boufford, J. I., Breyse, P. N., Chiles, T., Mahidol, C.,
1019 Coll-Seck, A. M., Cropper, M. L., Fobil, J., Fuster, V., Greenstone, M., Haines, A., Hanrahan, D.,
1020 Hunter, D., Khare, M., Krupnick, A., Lanphear, B., Lohani, B., Martin, K., Mathiasen, K. V.,
1021 McTeer, M. A., Murray, C. J. L., Ndahimananjara, J. D., Perera, F., Potočnik, J., Preker, A. S.,
1022 Ramesh, J., Rockström, J., Salinas, C., Samson, L. D., Sandilya, K., Sly, P. D., Smith, K. R.,
1023 Steiner, A., Stewart, R. B., Suk, W. A., van Schayck, O. C. P., Yadama, G. N., Yumkella, K. and
1024 Zhong, M.: The Lancet Commission on pollution and health, *Lancet*, 391(10119), 462–512,
1025 2018.

1026 Lelieveld, J., Evans, J. S., Fnais, M., Giannadaki, D. and Pozzer, A.: The contribution of outdoor
1027 air pollution sources to premature mortality on a global scale, *Nature*, 525(7569), 367–371, 2015.

1028 Liao, J., Hanisco, T. F., Wolfe, G. M., St. Clair, J., Jimenez, J. L., Campuzano-Jost, P., Nault, B.
1029 A., Fried, A., Marais, E. A., Gonzalez Abad, G., Chance, K., Jethva, H. T., Ryerson, T. B.,
1030 Warneke, C. and Wisthaler, A.: Towards a satellite formaldehyde – in situ hybrid estimate for
1031 organic aerosol abundance, *Atmos. Chem. Phys.*, 19(5), 2765–2785, 2019.

1032 Li, M., Zhang, Q., Zheng, B., Tong, D., Lei, Y., Liu, F., Chaopeng, H., Kang, S., Yan, L., Zhang,
1033 Y., Bo, Y., Su, H., Cheng, Y. and He, K.: Persistent growth of anthropogenic non-methane
1034 volatile organic compound (NMVOC) emissions in China during 1990-2017: drivers, speciation
1035 and ozone formation potential, *Atmos. Chem. Phys.*, 19, 8897–8913, 2019.

1036 Liu, X., Deming, B., Pagonis, D., Day, D. A., Palm, B. B., Talukdar, R., Roberts, J. M., Veres, P.
1037 R., Krechmer, J. E., Thornton, J. A., de Gouw, J. A., Ziemann, P. J. and Jimenez, J. L.: Effects of
1038 gas–wall interactions on measurements of semivolatile compounds and small polar molecules, ,
1039 doi:10.5194/amt-12-3137-2019, 2019.

1040 Lu, Q., Zhao, Y. and Robinson, A. L.: Comprehensive organic emission profiles for gasoline,
1041 diesel, and gas-turbine engines including intermediate and semi-volatile organic compound
1042 emissions, *Atmos. Chem. Phys.*, 18, 17637–17654, 2018.

1043 Ma, P. K., Zhao, Y., Robinson, A. L., Worton, D. R., Goldstein, A. H., Ortega, A. M., Jimenez, J.
1044 L., Zotter, P., Prévôt, A. S. H., Szidat, S. and Hayes, P. L.: Evaluating the impact of new
1045 observational constraints on P-S/IVOC emissions, multi-generation oxidation, and chamber wall
1046 losses on SOA modeling for Los Angeles, CA, *Atmos. Chem. Phys.*, 17(15), 9237–9259, 2017.

1047 McDonald, B. C., de Gouw, J. A., Gilman, J. B., Jathar, S. H., Akherati, A., Cappa, C. D.,
1048 Jimenez, J. L., Lee-Taylor, J., Hayes, P. L., McKeen, S. A., Cui, Y. Y., Kim, S.-W., Gentner, D.
1049 R., Isaacman-VanWertz, G., Goldstein, A. H., Harley, R. A., Frost, G. J., Roberts, J. M., Ryerson,
1050 T. B. and Trainer, M.: Volatile chemical products emerging as largest petrochemical source of
1051 urban organic emissions, *Science*, 359(6377), 760–764, 2018.

1052 Miyakawa, T., Takegawa, N. and Kondo, Y.: Photochemical evolution of submicron aerosol
1053 chemical composition in the Tokyo megacity region in summer, *J. Geophys. Res. D: Atmos.*,
1054 113(D14), D14304, 2008.

1055 Molina, L. T., Kolb, C. E., de Foy, B., Lamb, B. K., Brune, W. H., Jimenez, J. L.,
1056 Ramos-Villegas, R., Sarmiento, J., Paramo-Figueroa, V. H., Cardenas, B., Gutierrez-Avedoy, V.
1057 and Molina, M. J.: Air quality in North America's most populous city – overview of the
1058 MCMA-2003 campaign, *Atmos. Chem. Phys.*, 7(10), 2447–2473, 2007.

1059 Molina, L. T., Madronich, S., Gaffney, J. S., Apel, E., de Foy, B., Fast, J., Ferrare, R., Herndon,
1060 S., Jimenez, J. L., Lamb, B., Osornio-Vargas, A. R., Russell, P., Schauer, J. J., Stevens, P. S.,
1061 Volkamer, R. and Zavala, M.: An overview of the MILAGRO 2006 Campaign: Mexico City
1062 emissions and their transport and transformation, *Atmos. Chem. Phys.*, 10(18), 8697–8760,
1063 2010.

1064 Morino, Y., Tanabe, K., Sato, K. and Ohara, T.: Secondary organic aerosol model
1065 intercomparison based on secondary organic aerosol to odd oxygen ratio in Tokyo, *J. Geophys.*
1066 *Res.: Atmos.*, 119(23), 13,489–13,505, 2014.

1067 Murphy, B. N., Woody, M. C., Jimenez, J. L., Carlton, A. M. G., Hayes, P. L., Liu, S., Ng, N. L.,
1068 Russell, L. M., Setyan, A., Xu, L., Young, J., Zaveri, R. A., Zhang, Q. and Pye, H. O. T.:
1069 Semivolatile POA and parameterized total combustion SOA in CMAQv5.2: impacts on source
1070 strength and partitioning, *Atmos. Chem. Phys.*, 17(18), 11107–11133, 2017.

1071 Nault, B. A., Campuzano-Jost, P., Day, D. A., Schroder, J. C., Anderson, B., Beyersdorf, A. J.,
1072 Blake, D. R., Brune, W. H., Choi, Y., Corr, C. A., de Gouw, J. A., Dibb, J., DiGangi, J. P., Diskin,
1073 G. S., Fried, A., Huey, L. G., Kim, M. J., Knote, C. J., Lamb, K. D., Lee, T., Park, T., Pusede, S.
1074 E., Scheuer, E., Thornhill, K. L., Woo, J.-H. and Jimenez, J. L.: Secondary Organic Aerosol
1075 Production from Local Emissions Dominates the Organic Aerosol Budget over Seoul, South
1076 Korea, during KORUS-AQ, *Atmos. Chem. Phys.*, 18, 17769–17800, 2018.

1077 Pagonis, D., Krechmer, J. E., de Gouw, J., Jimenez, J. L. and Ziemann, P. J.: Effects of Gas-Wall
1078 Partitioning in Teflon Tubing and Instrumentation on Time-Resolved Measurements of
1079 Gas-Phase Organic Compounds, *Atmospheric Measurement Techniques Discussions*, 1–19,
1080 2017.

1081 Pai, S. J., Heald, C. L., Pierce, J. R., Farina, S. C., Marais, E. A., Jimenez, J. L.,
1082 Campuzano-Jost, P., Nault, B. A., Middlebrook, A. M., Coe, H., Shilling, J. E., Bahreini, R.,
1083 Dingle, J. H. and Vu, K.: An evaluation of global organic aerosol schemes using airborne

1084 observations, *Atmos. Chem. Phys.*, 20(5), 2637–2665, 2020.

1085 Parrish, D. D., Kuster, W. C., Shao, M., Yokouchi, Y., Kondo, Y., Goldan, P. D., de Gouw, J. A.,
1086 Koike, M. and Shirai, T.: Comparison of air pollutant emissions among mega-cities, *Atmos.*
1087 *Environ.*, 43(40), 6435–6441, 2009.

1088 Petit, J.-E., Favez, O., Sciare, J., Canonaco, F., Croteau, P., Močnik, G., Jayne, J., Worsnop, D.
1089 and Leoz-Garziandia, E.: Submicron aerosol source apportionment of wintertime pollution in
1090 Paris, France by double positive matrix factorization (PMF²) using an aerosol chemical
1091 speciation monitor (ACSM) and a multi-wavelength Aethalometer, *Atmos. Chem. Phys.*, 14(24),
1092 13773–13787, 2014.

1093 Platt, S. M., Haddad, I. E., Pieber, S. M., Huang, R.-J., Zardini, A. A., Clairotte, M.,
1094 Suarez-Bertoa, R., Barmet, P., Pfaffenberger, L., Wolf, R., Slowik, J. G., Fuller, S. J., Kalberer,
1095 M., Chirico, R., Dommen, J., Astorga, C., Zimmermann, R., Marchand, N., Hellebust, S.,
1096 Temime-Roussel, B., Baltensperger, U. and Prévôt, A. S. H.: Two-stroke scooters are a dominant
1097 source of air pollution in many cities, *Nat. Commun.*, 5(1), 3749, 2014.

1098 Pollack, I. B., Ryerson, T. B., Trainer, M., Neuman, J. A., Roberts, J. M. and Parrish, D. D.:
1099 Trends in ozone, its precursors, and related secondary oxidation products in Los Angeles,
1100 California: A synthesis of measurements from 1960 to 2010, *J. Geophys. Res. D: Atmos.*,
1101 118(11), 5893–5911, 2013.

1102 Pungler, E. M. and West, J. J.: The effect of grid resolution on estimates of the burden of ozone
1103 and fine particulate matter on premature mortality in the USA, *Air Qual. Atmos. Health*, 6(3),
1104 563–573, 2013.

1105 Ridley, D. A., Heald, C. L., Ridley, K. J. and Kroll, J. H.: Causes and consequences of
1106 decreasing atmospheric organic aerosol in the United States, *Proc. Natl. Acad. Sci. U. S. A.*,
1107 115(2), 290–295, 2018.

1108 Robinson, A. L., Donahue, N. M., Shrivastava, M. K., Weitkamp, E. A., Sage, A. M., Grieshop,
1109 A. P., Lane, T. E., Pierce, J. R. and Pandis, S. N.: Rethinking Organic Aerosols: Semivolatile
1110 Emissions and Photochemical Aging, *Science*, 315(5816), 1259–1262, 2007.

1111 Ryerson, T. B., Andrews, A. E., Angevine, W. M., Bates, T. S., Brock, C. A., Cairns, B., Cohen,
1112 R. C., Cooper, O. R., de Gouw, J. A., Fehsenfeld, F. C., Ferrare, R. A., Fischer, M. L., Flagan, R.
1113 C., Goldstein, A. H., Hair, J. W., Hardesty, R. M., Hostetler, C. A., Jimenez, J. L., Langford, A.
1114 O., McCauley, E., McKeen, S. A., Molina, L. T., Nenes, A., Oltmans, S. J., Parrish, D. D.,
1115 Pederson, J. R., Pierce, R. B., Prather, K., Quinn, P. K., Seinfeld, J. H., Senff, C. J., Sorooshian,
1116 A., Stutz, J., Surratt, J. D., Trainer, M., Volkamer, R., Williams, E. J. and Wofsy, S. C.: The 2010
1117 California Research at the Nexus of Air Quality and Climate Change (CalNex) field study, *J.*
1118 *Geophys. Res. D: Atmos.*, 118(11), 5830–5866, 2013.

1119 Sacks, J., Buckley, B., Alexis, N., Angrish, M., Beardslee, R., Benson, A., Brown, J., Buckley,
1120 B., Campen, M., Chan, E., Coffman, E., Davis, A., Dutton, S. J., Eftim, S., Gandy, J., Hemming,

1121 B. L., Hines, E., Holliday, K., Kerminen, V.-M., Kiomourtzoglou, M.-A., Kirrane, E., Kotchmar,
1122 D., Koturbash, I., Kulmala, M., Lassiter, M., Limaye, V., Ljungman, P., Long, T., Luben, T.,
1123 Malm, W., McDonald, J. F., McDow, S., Mickley, L., Mikati, I., Mulholland, J., Nichols, J.,
1124 Patel, M. M., Pinder, R., Pinto, J. P., Rappazzo, K., Richomond-Bryant, J., Rosa, M., Russell, A.,
1125 Schichtel, B., Stewart, M., Stanek, L. W., Turner, M., Van Winkle, L., Wagner, J., Weaver,
1126 Christopher, Wellenius, G., Whitsel, E., Yeckel, C., Zanobetti, A. and Zhang, M.: Integrated
1127 Science Assessment (ISA) for Particulate Matter (Final Report, Dec 2019), Environmental
1128 Protection Agency. [online] Available from:
1129 <https://cfpub.epa.gov/ncea/isa/recordisplay.cfm?deid=347534> (Accessed 20 October 2020),
1130 2019.

1131 Schroder, J. C., Campuzano-Jost, P., Day, D. A., Shah, V., Larson, K., Sommers, J. M., Sullivan,
1132 A. P., Campos, T., Reeves, J. M., Hills, A., Hornbrook, R. S., Blake, N. J., Scheuer, E., Guo, H.,
1133 Fibiger, D. L., McDuffie, E. E., Hayes, P. L., Weber, R. J., Dibb, J. E., Apel, E. C., Jaeglé, L.,
1134 Brown, S. S., Thornton, J. A. and Jimenez, J. L.: Sources and Secondary Production of Organic
1135 Aerosols in the Northeastern US during WINTER, *J. Geophys. Res. D: Atmos.*,
1136 doi:10.1029/2018JD028475, 2018.

1137 Seinfeld, J. H. and Pandis, S. N.: *Atmospheric Chemistry and Physics: From Air Pollution to*
1138 *Climate Change, Second.*, John Wiley & Sons, Inc., Hoboken, NJ USA., 2006.

1139 Seltzer, K. M., Pennington, E., Rao, V., Murphy, B. N., Strum, M., Isaacs, K. K. and Pye, H. O.
1140 T.: Reactive organic carbon emissions from volatile chemical products, *Atmos. Chem. Phys.*, 21,
1141 5079–5100, 2021.

1142 Shaddick, G., Thomas, M. L., Amini, H., Broday, D., Cohen, A., Frostad, J., Green, A., Gumy,
1143 S., Liu, Y., Martin, R. V., Pruss-Ustun, A., Simpson, D., van Donkelaar, A. and Brauer, M.: Data
1144 Integration for the Assessment of Population Exposure to Ambient Air Pollution for Global
1145 Burden of Disease Assessment, *Environ. Sci. Technol.*, 52(16), 9069–9078, 2018.

1146 Shah, V., Jaeglé, L., Thornton, J. A., Lopez-Hilfiker, F. D., Lee, B. H., Schroder, J. C.,
1147 Campuzano-Jost, P., Jimenez, J. L., Guo, H., Sullivan, A. P., Weber, R. J., Green, J. R., Fiddler,
1148 M. N., Bililign, S., Campos, T. L., Stell, M., Weinheimer, A. J., Montzka, D. D. and Brown, S.
1149 S.: Chemical feedbacks weaken the wintertime response of particulate sulfate and nitrate to
1150 emissions reductions over the eastern United States, *Proc. Natl. Acad. Sci. U. S. A.*, 115(32),
1151 8110–8115, 2018.

1152 Shah, V., Jaeglé, L., Jimenez, J. L., Schroder, J. C., Campuzano-Jost, P., Campos, T. L., Reeves,
1153 J. M., Stell, M., Brown, S. S., Lee, B. H., Lopez-Hilfiker, F. D. and Thornton, J. A.: Widespread
1154 Pollution from Secondary Sources of Organic Aerosols during Winter in the Northeastern United
1155 States, *Geophys. Res. Lett.*, doi:10.1029/2018GL081530, 2019.

1156 Shrivastava, M., Cappa, C. D., Fan, J., Goldstein, A. H., Guenther, A. B., Jimenez, J. L., Kuang,
1157 C., Laskin, A., Martin, S. T., Ng, N. L., Petaja, T., Pierce, J. R., Rasch, P. J., Roldin, P., Seinfeld,
1158 J. H., Shilling, J., Smith, J. N., Thornton, J. A., Volkamer, R., Wang, J., Worsnop, D. R., Zaveri,
1159 R. A., Zelenyuk, A. and Zhang, Q.: Recent advances in understanding secondary organic aerosol:

- 1160 Implications for global climate forcing, *Rev. Geophys.*, 55(2), 509–559, 2017.
- 1161 Silva, R. A., Adelman, Z., Fry, M. M. and West, J. J.: The Impact of Individual Anthropogenic
1162 Emissions Sectors on the Global Burden of Human Mortality due to Ambient Air Pollution,
1163 *Environ. Health Perspect.*, 124(11), 1776–1784, 2016.
- 1164 Singh, A., Satish, R. V. and Rastogi, N.: Characteristics and sources of fine organic aerosol over
1165 a big semi-arid urban city of western India using HR-ToF-AMS, *Atmos. Environ.*, 208, 103–112,
1166 2019.
- 1167 Stavroulas, I., Bougiatioti, A., Grivas, G., Paraskevopoulou, D., Tsagkaraki, M., Zarnpas, P.,
1168 Liakakou, E., Gerasopoulos, E. and Mihalopoulos, N.: Sources and processes that control the
1169 submicron organic aerosol composition in an urban Mediterranean environment (Athens): a high
1170 temporal-resolution chemical composition measurement study, *Atmos. Chem. Phys.*, 19(2),
1171 901–919, 2019.
- 1172 Stewart, G. J., Nelson, B. S., Acton, W. J. F., Vaughan, A. R., Farren, N. J., Hopkins, J. R., Ward,
1173 M. W., Swift, S. J., Arya, R., Mondal, A., Jangirh, R., Ahlawat, S., Yadav, L., Sharma, S. K.,
1174 Yunus, S. S. M., Hewitt, C. N., Nemitz, E., Mullinger, N., Gadi, R., Sahu, L. K., Tripathi, N.,
1175 Rickard, A. R., Lee, J. D., Mandal, T. K. and Hamilton, J. F.: Emissions of intermediate-volatility
1176 and semi-volatile organic compounds from domestic fuels used in Delhi, India, *Atmos. Chem.*
1177 *Phys. Discuss.*, doi:10.5194/acp-2020-860, 2020.
- 1178 Toon, O. B., Maring, H., Dibb, J., Ferrare, R., Jacob, D. J., Jensen, E. J., Luo, Z. J., Mace, G. G.,
1179 Pan, L. L., Pfister, L., Rosenlof, K. H., Redemann, J., Reid, J. S., Singh, H. B., Thompson, A.
1180 M., Yokelson, R., Minnis, P., Chen, G., Jucks, K. W. and Pszenny, A.: Planning, implementation,
1181 and scientific goals of the Studies of Emissions and Atmospheric Composition, Clouds and
1182 Climate Coupling by Regional Surveys (SEAC⁴RS) field mission, *J. Geophys. Res. D: Atmos.*,
1183 121(9), 4967–5009, 2016.
- 1184 Tsimpidi, A. P., Karydis, V. A., Zavala, M., Lei, W., Molina, L., Ulbrich, I. M., Jimenez, J. L. and
1185 Pandis, S. N.: Evaluation of the volatility basis-set approach for the simulation of organic aerosol
1186 formation in the Mexico City metropolitan area, *Atmos. Chem. Phys.*, 10(2), 525–546, 2010.
- 1187 Volkamer, R., Jimenez, J. L., San Martini, F., Dzepina, K., Zhang, Q., Salcedo, D., Molina, L. T.,
1188 Worsnop, D. R. and Molina, M. J.: Secondary organic aerosol formation from anthropogenic air
1189 pollution: Rapid and higher than expected, *Geophys. Res. Lett.*, 33(17), L17811, 2006.
- 1190 Wang, L., Slowik, J. G., Tripathi, N., Bhattu, D., Rai, P., Kumar, V., Vats, P., Satish, R.,
1191 Baltensperger, U., Ganguly, D., Rastogi, N., Sahu, L. K., Tripathi, S. N. and Prévôt, A. S. H.:
1192 Source characterization of volatile organic compounds measured by proton-transfer-reaction
1193 time-of-flight mass spectrometers in Delhi, India, *Atmos. Chem. Phys.*, 20(16), 9753–9770,
1194 2020.
- 1195 Warneke, C., de Gouw, J. A., Holloway, J. S., Peischl, J., Ryerson, T. B., Atlas, E., Blake, D.,
1196 Trainer, M. and Parrish, D. D.: Multiyear trends in volatile organic compounds in Los Angeles,

1197 California: Five decades of decreasing emissions, *J. Geophys. Res. D: Atmos.*, 117(D21),
1198 D00V17, 2012.

1199 Wood, E. C., Canagaratna, M. R., Herndon, S. C., Onasch, T. B., Kolb, C. E., Worsnop, D. R.,
1200 Kroll, J. H., Knighton, W. B., Seila, R., Zavala, M., Molina, L. T., Decarlo, P. F., Jimenez, J. L.,
1201 Weinheimer, A. J., Knapp, D. J., Jobson, B. T., Stutz, J., Kuster, W. C. and Williams, E. J.:
1202 Investigation of the correlation between odd oxygen and secondary organic aerosol in Mexico
1203 City and Houston, *Atmos. Chem. Phys.*, 10(18), 8947–8968, 2010.

1204 Woody, M. C., Baker, K. R., Hayes, P. L., Jimenez, J. L., Koo, B. and Pye, H. O. T.:
1205 Understanding sources of organic aerosol during CalNex-2010 using the CMAQ-VBS, *Atmos.*
1206 *Chem. Phys.*, 16(6), 4081–4100, 2016.

1207 Worton, D. R., Isaacman, G., Gentner, D. R., Dallmann, T. R., Chan, A. W. H., Ruehl, C.,
1208 Kirchstetter, T. W., Wilson, K. R., Harley, R. A. and Goldstein, A. H.: Lubricating Oil Dominates
1209 Primary Organic Aerosol Emissions from Motor Vehicles, *Environ. Sci. Technol.*, 48(7),
1210 3698–3706, 2014.

1211 Ye, P., Ding, X., Hakala, J., Hofbauer, V., Robinson, E. S. and Donahue, N. M.: Vapor wall loss
1212 of semi-volatile organic compounds in a Teflon chamber, *Aerosol Sci. Technol.*, 50(8), 822–834,
1213 2016.

1214 Zhang, Q., Jimenez, J. L., Canagaratna, M. R., Allan, J. D., Coe, H., Ulbrich, I., Alfarra, M. R.,
1215 Takami, A., Middlebrook, A. M., Sun, Y. L., Dzepina, K., Dunlea, E., Docherty, K., DeCarlo, P.
1216 F., Salcedo, D., Onasch, T., Jayne, J. T., Miyoshi, T., Shimono, A., Hatakeyama, S., Takegawa,
1217 N., Kondo, Y., Schneider, J., Drewnick, F., Borrmann, S., Weimer, S., Demerjian, K., Williams,
1218 P., Bower, K., Bahreini, R., Cottrell, L., Griffin, R. J., Rautiainen, J., Sun, J. Y., Zhang, Y. M. and
1219 Worsnop, D. R.: Ubiquity and dominance of oxygenated species in organic aerosols in
1220 anthropogenically-influenced Northern Hemisphere midlatitudes, *Geophys. Res. Lett.*, 34(13),
1221 L13801, 2007.

1222 Zhang, Q. J., Beekmann, M., Freney, E., Sellegri, K., Pichon, J. M., Schwarzenboeck, A.,
1223 Colomb, A., Bourriane, T., Michoud, V. and Borbon, A.: Formation of secondary organic
1224 aerosol in the Paris pollution plume and its impact on surrounding regions, *Atmos. Chem. Phys.*,
1225 15(24), 13973–13992, 2015.

1226 Zhao, B., Wang, S., Donahue, N. M., Jathar, S. H., Huang, X., Wu, W., Hao, J. and Robinson, A.
1227 L.: Quantifying the effect of organic aerosol aging and intermediate-volatility emissions on
1228 regional-scale aerosol pollution in China, *Sci. Rep.*, 6, 28815, 2016a.

1229 Zhao, Y., Hennigan, C. J., May, A. A., Daniel, S., Gouw, J. A. D., Gilman, J. B., Kuster, W. C.
1230 and Robinson, A. L.: Intermediate-Volatility Organic Compounds: A Large Source of Secondary
1231 Organic Aerosol, *Environ. Sci. Technol.*, 48(23), 13743–13750, 2014.

1232 Zhao, Y., Nguyen, N. T., Presto, A. A., Hennigan, C. J., May, A. A. and Robinson, A. L.:
1233 Intermediate Volatility Organic Compound Emissions from On-Road Gasoline Vehicles and

1234 Small Off-Road Gasoline Engines, *Environ. Sci. Technol.*, 50(8), 4554–4563, 2016b.

1235 Zhao, Y., Saleh, R., Saliba, G., Presto, A. A., Gordon, T. D., Drozd, G. T., Goldstein, A. H.,

1236 Donahue, N. M. and Robinson, A. L.: Reducing secondary organic aerosol formation from

1237 gasoline vehicle exhaust, *Proc. Natl. Acad. Sci. U. S. A.*, 114(27), 6984–6989, 2017.

1238